

REPUBLIC OF TURKEY
AYDIN ADNAN MENDERES UNIVERSITY
GRADUATE SCHOOL OF NATURAL AND APPLIED SCIENCES
MECHANICAL ENGINEERING
2020-M.Sc.-007



**POWER CONSUMPTION REDUCTION STUDIES
AND ANALYSIS FOR CENTRIFUGAL
SEPARATOR**

Erdem SAĞLAM

Supervisor:
Prof. Dr. Yunus ÇERÇİ

AYDIN

REPUBLIC OF TURKEY
AYDIN ADNAN MENDERES UNIVERSITY
GRADUATE SCHOOL OF NATURAL AND APPLIED SCIENCES
AYDIN

The thesis with the title of “POWER CONSUMPTION REDUCTION STUDIES AND ANALYSIS FOR CENTRIFUGAL SEPARATOR” prepared by the MSc Candidate Erdem SAĞLAM at the MSc Program at the Department of Mechanical Engineering was accepted by the jury members whose names and titles presented below as a result of thesis defense on 14/01/2020.

	Title, Name Surname	Institution	Signature
President :	Prof. Dr. Yunus ÇERÇİ	Aydın Adnan Menderes University	
Member :	Asst. Prof. Dr. Adem ÖZÇELİK	Aydın Adnan Menderes University	
Member :	Asst. Prof. Dr. Ali YURDDAŞ	Manisa Celal Bayar University	

This Master Thesis accepted by the jury members is endorsed by the decision of the Institute Board Members with <.....> Serial Number and <.....> date.

Prof. Dr. Gönül AYDIN
Institute Director

REPUBLIC OF TURKEY
AYDIN ADNAN MENDERES UNIVERSITY
GRADUATE SCHOOL OF NATURAL AND APPLIED SCIENCES
AYDIN

I hereby declare that all information and results reported in this thesis have been obtained by my part as a result of truthful experiments and observations carried out by the scientific methods, and that I referenced appropriately and completely all data, thought, result information which do not belong my part within this study by virtue of scientific ethical codes.

14/01/2020

Erdem SAĞLAM

ÖZET

SANTRİFÜJ SEPARATÖRDE ENERJİ TÜKETİMİ AZALTIM ÇALIŞMALARI VE ANALİZİ

Erdem SAĞLAM

Yüksek Lisans Tezi, Makine Mühendisliği Anabilim Dalı

Tez Danışmanı: Prof. Dr. Yunus ÇERÇİ

2020, 56 sayfa

Santrifüj separatörlerin güç tüketimini etkileyen faktörler; tambur dış yüzeyindeki hava sürtünmesi, hareketli parçalardaki sürtünmeden kaynaklı mekanik kayıplar, elektriksel kayıplar ve akış kayıpları olmak üzere dört ana başlık altında toplanabilir. Bu başlıklar altında güç tüketimini etkileyen parametreler detaylıca irdelenmiştir. Toplam güç tüketiminin %32'si tambur dış yüzeyindeki hava sürtünmesine, %9'u mekanik kayıplara, %10'u elektriksel kayıplara ve %49'u akışı hızlandırmak için harcadığı tespit edilmiştir ve diğer bileşenler arasında en büyük güç tüketimini oluşturmaktadır. Separasyon verimini azaltmadan, açısız momentumdan kaynaklanan güç tüketiminin düşürülmesi için ana faktör olarak merkezci pompa tasarımına odaklanılmıştır. Optimize edilmiş merkezci pompa ile metreküp başına güç tüketimi 0,99 kWh m⁻³ değerine düşürülmüş olup %12 oranında azaltılması sağlanmıştır.

Anahtar Kelimeler: Santrifüj separatör, güç tüketimi, merkezci pompa

ABSTRACT**POWER CONSUMPTION REDUCTION STUDIES AND ANALYSIS FOR CENTRIFUGAL SEPARATOR**

Erdem SAĞLAM

M.Sc. Thesis, Department of Mechanical Engineering

Supervisor: Prof. Dr. Yunus ÇERÇİ

2020, 56 pages

The factors affecting the power consumption of centrifugal separators can be grouped under four main headings. These are air friction on the outer surface of bowl group, mechanical losses due to friction on moving parts, electrical losses and flow losses. The parameters affecting the power consumption are examined in detail under these headings. It has been found that 32% of the total power consumption is spent to overcome the air friction on the outer surface of bowl group, 9% to mechanical losses, 10% to electrical losses and 49% to accelerate the flow and constitutes the biggest consumption among the other power components. The main factor for reducing power consumption due to angular momentum without reducing separation efficiency is the focus on centripetal pump design. With the optimized centripetal pump, the power consumption per cubic meter has been reduced to 0.99 kWh m^{-3} and 12% reduction in total power consumption was achieved.

Key Words: Centrifugal separator, power consumption, centripetal pump

ACKNOWLEDGEMENTS

I would like to thank my family for believing in me and supporting me throughout my career at Aydın Adnan Menderes University. I would also like to thank my supervisor, Prof. Dr. Yunus ÇERÇİ for their support and guidance while working on my thesis. I am grateful to Mr. Hakkı GÖZLÜKLÜ, our general manager who opened the way for me in my study on the centrifugal separator which forms the basis of my thesis.

Erdem SAĞLAM

TABLE OF CONTENTS

ÖZET.....	vii
ABSTRACT.....	ix
ACKNOWLEDGEMENTS.....	xi
1 INTRODUCTION.....	1
1.1 Disc Stack Centrifugal Separators.....	1
1.2 High Energy Consumption of Centrifugal Separators.....	2
2 LITERATURE REVIEW.....	4
3 MATERIAL AND METHOD.....	10
3.1 Configuration and Operating Principles of Centrifugal Separators.....	10
3.2 Determination of the Main Factors Influencing the Power Consumption ...	12
3.2.1 Idle Power Consumption.....	13
3.2.1.1 Power loss due to air friction (windage).....	14
3.2.1.2 Mechanical losses.....	16
3.2.2 Flow Losses.....	19
3.2.3 Electrical Losses.....	21
3.3 Theory of Centripetal Pump.....	23
3.4 Field Test Unit.....	27
3.5 Centripetal Pump Simulations in CFD.....	30
3.5.1 Problem Definition.....	30
3.5.2 Model Properties.....	33

3.5.3 Mesh Structure	34
3.5.4 CFD Setup on Fluent Solver.....	37
4 RESULTS AND DISCUSSIONS	40
4.1 Main Factors of Power Consumption.....	40
4.2 Validation of Power Recovery Through the Centripetal Pump.....	44
5 CONCLUSION	51
REFERENCES	53
RESUME.....	55

LIST OF SYMBOLS

ρ	: Density
P	: Pressure
P_{total}	: Total power consumption
r_b	: Radius of a bowl
r_c	: Radius of a centripetal pump
F_1	: Tensional force on tight side
F_2	: Tensional force on slack side
n	: Revolution per minute
T	: Torque
θ	: Total contact angle of belt on pulley
ω, Ω	: Angular velocity
P_c	: Centrifugal force acting on a belt
Q	: Throughput rate
v	: Speed
t_{cm}	: Time for one circular motion
μ_b	: Coefficient of friction between a belt and a pulley
m_b	: Unit mass of a belt
η	: Efficiency
\dot{L}	: Angular momentum
\dot{p}	: Linear momentum

Q_v : Volumetric flowrate

c_f : Coefficient of Friction

P_{rec} : Recovered Power by a Centripetal Pump

e : Euler's Number

k : Turbulence kinetic energy

ε : Turbulence dissipation rate

Re : Reynolds Number

LIST OF ABBREVIATIONS

<u>Abbreviation</u>	<u>Expansion of the Term</u>
VFD	: Variable Frequency Drive
HMI	: Human Machine Interface
MCC	: Motion Control Center
CAD	: Computer Aided Drawing
CAE	: Computer Associated Engineering
CFD-DEM	: Computational Fluid Dynamics-Discrete Element Modeling
RANS	: Reynolds Averaged Navier-Stokes
RNG	: Renormalization Group
CIP	: Cleaning in Place
MRF	: Moving Reference Model
URF	: Under-Relaxation Factors

LIST OF FIGURES

Figure 1.1 Photograph (left) of an ejecting, self-cleaning, disc stack centrifuge. Also shown (right) is a typical disc stack bowl (Courtesy of HAUS Centrifuge Technologies).....	2
Figure 3.1: Cross section view of the bowl group of a Maxcream 30T centrifugal separator. (Courtesy of HAUS Centrifuge Technologies, 2019).	11
Figure 3.2: The distributor with a disc stack on it.....	11
Figure 3.3: Power consumption rate of a standard dairy separator at different flow rates. (Courtesy of HAUS Centrifuge Technologies)	13
Figure 3.4: Exterior of the bowl group of the testing separator centrifugal separator divided into sub parts.	14
Figure 3.5: Belt drive mechanism	17
Figure 3.6: The components of electrical panel	21
Figure 3.7: Speed-time chart of a VFD (high)	22
Figure 3.8: Speed-time chart of a VFD (low)	22
Figure 3.9: Label of the electrical motor.....	23
Figure 3.10: A centripetal pump and the flow. (HAUS Centrifuge Technologies, 2019)	24
Figure 3.11: The stationary centripetal pump	24
Figure 3.12: The testing setup in R&D Testing Field	27
Figure 3.13: The VFD of the feed pump.....	28
Figure 3.14: A photograph of the flowmeter.....	29
Figure 3.15: Centripetal pumps before assembling the separator.	29

Figure 3.16: 3D Models of the centripetal pumps	30
Figure 3.17: Cross section of a centripetal pump.	31
Figure 3.18: The 3D models of centripetal pumps and the difference in channel designs.....	32
Figure 3.19: CFD model evolution from SolidWorks CAD to meshing.....	34
Figure 3.20: Mesh characteristics of 150 mm diameter, six channel centripetal pump with tetra mesher.	35
Figure 3.21: CFD Solver residual monitor at the step of convergence	39
Figure 4.1: Power consumption of centripetal pump variations at 2 bar counter pressure.....	40
Figure 4.2: Power consumption of centripetal pumps at 26 m ³ /h throughput rate	41
Figure 4.3: Distribution of Power Consumption of the Testing Separator.....	44
Figure 4.4: Pressure distribution through 150 mm (top, left), 160 mm (top, right) and 170 mm centripetal pump designs in k-Ω RANS model.	46
Figure 4.5: Vector graph for velocity distribution along 150 mm (top,left), 160 mm (top,right) and 170 mm centripetal pump designs in k-Ω RANS model.....	47
Figure 4.6: Pump pressure losses at 2 bar counter pressure	48
Figure 4.7: Pump pressure losses at 26 m ³ /h throughput rate.....	48
Figure 4.8: Power recycled from centripetal pumps at 2 bar counter pressure	49
Figure 4.9: Power recycled from centripetal pumps at 26 m ³ /h throughput rate...	49
Figure 4.10: Recovered power by centripetal pumps at 26 m ³ /h throughput rate .	50

LIST OF TABLES

Table 3.1: The areas are collected from the measure feature of the Solidworks CAD software.....	33
Table 3.2: Mesh properties applied to each model.....	36
Table 3.3: Solution methods group utilized through the simulations.....	37
Table 3.4: Standard initialization values for nominal speed and pointwise simulation parameters	38
Table 4.1: Distribution of power consumption factors.....	43

1 INTRODUCTION

Mechanical separation is a method that has been used for years to separate liquid mixtures or to separate solids from a liquid or liquid mixture. If the density difference between the liquids is sufficient, gravity can be used as a mechanical separation method. As the gravitational force increases, the time required for mechanical separation reduces. Industrial devices like decanters and separators have been designed to use this principle by creating an artificial gravitational force. These devices known as energy hungry machinery due to their relatively high-power needs. The aim of this study is to address the factors of energy consumption of centrifugal separators and reducing the overall energy consumption by making certain design modifications.

1.1 Disc Stack Centrifugal Separators

Disc stack centrifuge is a versatile device, which may be used for separating solid/liquid mixtures in continuous, semi-continuous and batch configurations. All except some batch operated machines are able to handle toxic, flammable and volatile feeds at throughputs up to 200 m³/h.

Liquid-liquid mixtures can be separated and with more sophisticated units a three (two liquid and one solid) phase separation is achievable. In all cases, a sufficient density difference must exist between the phases present in the feed.

Although several variants exist, the generic type is characterized by an imperforate bowl surrounding an inverted stack of thin conical discs separated by 0.3-3 mm spacers. The disc spacing is dependent on the viscosities and solids concentrations favor spacing below 1 mm. As the discs are spun on a common vertical axis the process suspension, which is fed centrally from top, travels through the annular spaces between the discs.

Centrifugal forces up to 14000g cause particles to accumulate on the underside of the discs from where they slide down towards the outer periphery of centrifuge bowl. In batch units the thickened solids remain in the bowl until the solids handling capacity of the centrifuge is reached. At this point rotation stops and the basket containing the trapped solids is manually replaced or a discharge valve on the periphery of the bowl is manually operated to facilitate removal of the

sediment. In continuous units the solids, which must be flowable, is automatically separate at periodic intervals and discharge the accumulated solids.



Figure 1.1 Photograph (left) of an ejecting, self-cleaning, disc stack centrifuge. Also shown (right) is a typical disc stack bowl (Courtesy of HAUS Centrifuge Technologies)

While disc stack centrifuges are able to accept a wide range of feeds, they are both mechanically complex and expensive. Moreover, the close stacking of conical discs means that mechanical cleaning can be difficult, and resort is often made to chemical cleaning (Tarleton, E.S. & Wakeman, R.J., 2007).

1.2 High Energy Consumption of Centrifugal Separators

Currently most of the centrifugal separators operate at a rate around 1.2 kWh m^{-3} or sometimes up to 1.5 kWh m^{-3} so this level of power consumption raises new debates about power efficiency. Increasing energy costs put forward the idea that the energy efficiency of not only vehicles or small devices but also industrial machines should be increased.

Electrical power which is supplied to the separator is mostly used for rotating the bowl group therefore applying rotational force to the continuous fluid. Devices such as HMI (human machine interface) or safety equipment attached to the separator frame also consumes power but not much can be done about them to

reduce energy consumption. Increasing the efficiency to reduce the power consumption of a centrifugal separator could be possible by reducing the power losses. To increase the efficiency of a centrifugal separator, the main factors of power consumption must be determined. Once the factors have been identified, it would be appropriate to make changes to one of the conditions leading to high consumption. Changing the design of a part might be highly effective in reducing power consumption. In this study, firstly the situations that cause high power consumption will be determined by following the approach explained above and then the effects of design changes on power consumption will be observed.

2 LITERATURE REVIEW

The industrial centrifuge machinery's designs came a long way from the design of the first industrial cream separator invented by Gustaf de Laval in 1878. The design changes for better product feeding, faster rotation, better separation efficiency and easy cleaning of the centrifuge device are the factors of which the most innovations made in the sector. Sutherland (2009) carefully summarizes the history of the centrifuge machinery. He explains that the market share of the centrifuge devices is mostly acquired by the GEA Westfalia and the Alfa Laval corporations and the design of the centrifuge machines have changed along the years by the technological advancements like better discharging systems. The manufacturer's made significant improvements on centrifuge devices like the discharging systems that opens the bowl group to clean the centrifuge from the and an improved feed pipe system to lower the shear stress on the product. The competition between the manufacturers has become more and more challenging because of huge number of manufacturers started to develop centrifuge machinery over the world.

The changes that made by the manufacturers in the race to increase market share accelerated with the development of technology and at the same time improved the technology. Choosing a centrifuge separator or decanter is becoming harder every day because of the advancements in design of those machines like bigger capacity and lower running cost. The running cost consists of the resource that consumed by the separator during operating. One of the resources is water which is used by most of the centrifuge separators as a hydraulic fluid to open solenoid valves and such. The other resource is the electricity itself. Electric motors which powers the centrifugal separators or decanters are the core element of the centrifuge machinery. The increase of the motor power gives the ability to increase the separation capacity, but it also increases the power consumption of the machine. The drive mechanism and electrical equipment on centrifuge machines also draws power and they all add up really fast. Today's centrifuge separators can use 1 kWh m⁻³ or more during operation depend on a process and the cost effectiveness of the centrifuge separators and decanters are started to be discussed by customers. The electric motor is the core of the centrifuge and it can be hard to make improvements on the motor. The power transmission however can be designed better to be more efficient like belt drive mechanism instead of gear drive

mechanism. In fact, the newest drive mechanism named direct drive technology also raises the bar of efficiency challenge by being more power efficient than belt drive. In traditional electric motors, drive mechanisms such as belt drive and gear drive are widely used because of the insufficient speed of the motors. On the other hand, direct drive motors can provide more revolutionary speed. Therefore, no drive mechanism is required. Using a drive mechanism causes power loss about 5-10% of the delivered power for gear drive mechanism and 2% of the delivered power for belt drive mechanism. Because of that separators with direct drive motors are more power efficient. A common misconception about direct-drive motors is that the higher speed of the motors causes more aerodynamic drag, but these losses are small and can be ignored. Also, the commonly used drive mechanisms are causing even more aerodynamical drag by high speed rotating pulleys and gears. With these drag forces in mind it is possible to say that the power loss when using belt drive mechanism might be 3% of the delivered power. The design of the direct drive motors is quite different from traditional electrical motors. They are designed to be used with a VFD (variable frequency drive). This provides lower power loss for the use of a VFD and provides 95% efficiency for the combination of motor and VFD. It is a major improvement from 91% efficiency for combination of traditional motors and a VFD.

The chase of efficiency has become an important challenge among the machine manufacturers these days. With the increase of energy costs, a new factor introduced to the competition between the manufacturers of centrifugal separator. Centrifugal separators are commonly used equipment for tons of applications among sectors from food to industrial fluids. Separating mixtures to its phases to be able to gather valuable resources like cream of the milk and the fat of the fish is the main objective of these centrifuge machinery. From engineering standpoint, the centrifuge separators are hard to manufacture thereby expensive solutions for various processes. Even disregarding the separator's buying cost, the running cost of the centrifuge separators are huge compared to the other machinery in a process. The "running cost of a centrifuge separator to gained overall profit" ratio is very low at some sectors like biodiesel manufacturing from microalgae. In his recent study Milledge addressed the problem of high running cost of disc stack centrifuge separators which are working in microalgae harvesting sector (Milledge, J. & Heaven, S., 2011). The term biofuel was also frequently heard throughout the search for renewable power source and microalgae is one of the

popular biofuel sources. Milledge carefully explained the steps of gathering biofuel by harvesting microalgae and he inspected the process from an economic standpoint. As an example, a Westfalia HSB400 disc stack centrifugal separator's maximum motor power is 75 kW and the maximum capacity of it is 95 m³/h. The centrifugal separator's capacity heavily depends on a process thus the HSB400's capacity for microalgae harvesting becomes 35 m³/h at most. Therefore, the running cost of the separator becomes around 1.4 kWh m⁻³, which is not cost effective for its process. If a dry weight of 0.02% algae-water suspension is fed into the centrifugal separator, roughly 1.4 kg of algal oil and 7 kg of dry algal material can be gathered. Even if 90% of the algal oil is converted to methyl ester biodiesel the calorific value of the generated energy is too low compared to the separator's power consumption. Other studies also stated that the running costs of centrifugation is quite high. Verma et al. (2010) mentions to the high running costs of harvesting microalgae by centrifugation and the process efficiency is not at desirable levels.

The HSB400 separator which is mentioned by Milledge is not the only separator solution with high running costs but for microalgae harvesting process, other centrifuge separator manufacturers are also stating around the same amount of power consumption. Process efficiency of a centrifuge separator seem low for some processes but one of the main factors which affects process efficiency are the capacity and the power consumption. Therefore, the process efficiency might be higher for same centrifuge machine when working with different products since separation capacity is heavily tied with the fluid properties

In centrifugal separators, one of the biggest shares of a low process efficiency is belong to the high-power consumption. For example, even when the centrifuge separator is not processing the product, the current drawn is too high, because of speed up the whole bowl group to operating speed. A number of ways comes to mind for increasing the process efficiency. A centrifuge separator consists of a frame construction, a rotating bowl, a drive mechanism and an electrical motor. Lowering the power amount consumed by the electric motor can be effective for increasing the process efficiency. Increasing the capacity of the centrifuge separator also will make the process efficiency higher than before. The power of the motor is transmitted by a drive mechanism and the high mechanical losses of drive mechanisms are known facts. Using more efficient equipment such as the high efficiency electrical motors and more efficient drive mechanisms can also

increase the process efficiency. In his recent study, Khalid (2014), investigated the problem of costs of power consumption on electrical machinery and accessories. In his study, it is emphasized that it became more and more crucial over the last few years for the manufacturers of various electrical equipment to investigate on better solutions regarding minimization of power losses without risking from the efficiency. In this perspective, the VFD's (variable frequency drive) have come into spotlight where a myriad of applications is converted to operate on them in a range from small household devices to largest of mining mill drives. Centrifuge technologies in the last decade started to take advantage of these devices as well. In his study Friso (2017) inspected the centrifugation process to make numeric and experimental measurements of the benefits of using a VFD instead of a traditional system with a gearbox on centrifuge devices. The dynamic analysis of the gearbox system is conducted and compared to a VFD system without gearbox. Therefore, machine's starting times and speeds are compared. Lower starting time has been achieved by using a VFD instead of a gearbox. Also, the numerical approach to the designs shown a correlation between the starting time and the electric motor power. To reduce the starting time of the machine even more, electrical motor has been overloaded and the results are also compared to the previous findings. Thus, the study concludes on a lower starting time and reduced investment costs can be achievable.

Making design changes in the way of reducing the power consumption of a centrifuge machinery might be tried if the separation theory and the centrifuge machinery is well understood. The consumed power can be listed in subcategories to examine it easily. In his PhD thesis study Bell (2013) has investigated a decanter which is a centrifuge machinery with its immense details. The performance of decanter has been researched and the parameters have been classified step by step carefully. He also took a numerical approach and shares the detailed calculations of each step. The parameters which cause power losses are determined and the optimization actions has been taken along the study. He also stated that the feed acceleration cannot be underestimated for the operation of a decanter centrifuge. Insufficient acceleration can have a various of undesirable effects on the operation. The two major components of the insufficient feed acceleration have been stated under the viscous losses and the loss of kinetic energy topics. The transmission losses are made up of inefficiencies in the motors, belt drives, gearbox, bearings, and seals. The calculated total combined

transmission losses in decanters are 14 % of the total power input when the centrifuge is fully loaded. When the centrifuge is loaded to 50% the transmission losses were 21% of the total power consumption. The findings state that the windage losses due to air friction of rotating bowl is account for approximately 2% of the total power consumption. The magnitude of the windage losses does not vary with load, only with speed. Windage of the high-speed rotating bowl also cause high noise during operation, so the benefits of reducing the windage losses will also reduce the noise of the decanter. After operating the decanter for long time period, the power which required to accelerate the bowl to operating speed becomes insignificant compared to other losses. Also, lighter bowl group can increase the bearing life to reduce maintenance costs. At last chapters of his work, he made a CFD analysis of the bowl group to investigate the fluid behavior and the torque. The predicted fluid behavior and the high-speed photography compared to understand that they are in correlation. The work an achievement in the way of understanding the decanter technology.

The centrifuge machinery can also be used for other phase separations for example gas-liquid separation. The designs are clearly different than the centrifugal disc stack separator, but the mechanical separation principle is still the key. Kefalas and Margaris (2009) researched a separator which is commonly used for separation of mixtures like air and water. The investigations of a brand-new centrifugal phase separator have been modeled and various CFD analyses have been computed by them. The separator is comprised of an inlet and an outlet volute which is also connected to a cylindrical tower to maintain an equal phase separation by centrifugal forces. Thanks to the different mesh structures and mesh resolutions, the analysis by using RNG $k-\epsilon$ turbulence model achieved tangible results. The usage of a realistic centrifugal phase separator as a guide provided a geometrically correct 3D model and it enhanced the correlation of the experimental data with the analysis.

High speed rotation of the centrifugal separator's bowl is another cause of the low efficiency. The air volume between the bowl and the upper case of the separator is constantly creating an air friction, which in theory can be reduced by achieving a vacuum environment. The industrial design of the separator does not allow vacuum environment, but this does not mean the windage effect can not be examined. Such study has been done by the Wild and Djilali (1996) and they investigated a Couette Flow between a fixed enclosure and a rotating, co-centric

body of a centrifugal desalinators which involves both the flow in the annular and through the axial gap domain. It is suggested that, the flow field displays a remarkable variety along the axial distribution of the shear stress because of the secondary flow, according to computational simulations. It has also been outlined that smaller rotor length to radial gap proportions cause a higher median shear stresses when compared to cases where this proportion is relatively larger. In the study, relative research on the power law relations are also investigated for different formulae for windage moments of infinite cylinders. Several studies are discovered to be relevant with the experimental data. These discussed relations are found to be the most useful where the optimization of any rotating equipment, i.e. centrifugal device.

Tubular bowl, chamber bowl, imperforate basket, disc stack separator and decanters are various designs of a centrifuge technology mainly used in diverse applications (Sutherland, 2009). The decanters and the separators have much in common but the main design of these two is very different. The decanter has a horizontal rotating bowl and it is commonly used in a separation of high solid content mixtures. Unlike decanters, separators have vertical rotating bowl with a different shape, and they are used in separation of low solid content mixtures. The decanters have more source on design and calculations than separators in the literature. One of the main aims of this study is also creating another scientific study related to centrifugal separators. Thus, expanding the range of power-saving applications on the subject one step further.

3 MATERIAL AND METHOD

3.1 Configuration and Operating Principles of Centrifugal Separators

Disc stack centrifugal separators operate to constantly separate solid particles contained in fluids and/or fluid phases by using the centrifugal force. There are different types of disc stack centrifugal separators, but one of the design differences is the method of removal of solids. The manual cleaning separators do not remove the solids in the bowl automatically and they need a cleaning operation which involves disassembly of the whole machine. The automatic cleaning separators on the other hand has a discharge system which is used for removal of the solid accumulation inside the bowl.

In most popular discharge system, the piston inside the bowl is designed to be able to move vertically for opening the discharge ports during operation to remove solids. Water is used for hydraulic trigger in these discharge systems and solid discharge interval is determined by the solid particle amount contained in the fluid. The other discharge system is nozzle discharge system. In nozzle discharge systems, the bowl is designed to have a series of nozzles attached to its periphery so that a continuous discharge of the solids ensured.

Centrifugal separators categorized as clarifier, purifier and concentrator according to the application they are designed to operate. The clarifiers are used specially for removal of solids from fluid or fluid mixtures. The purifier and concentrator are used to separate the fluid mixtures into phases. While separating the phases they are also effective at cleaning the solids accumulation inside bowl by discharging solids at certain intervals. In each centrifugal separator configuration, design of the chamber group within the separator varies greatly.

To better understand the disc stack centrifugal separators, the following Figure 3.1 which shows a cross section view of the bowl group of a HAUS Maxcream 30T centrifugal separator has been shared. The Maxcream 30T model is hereinafter referred to as the 'testing separator' and is the model in which calculations and experiments are performed for this study.

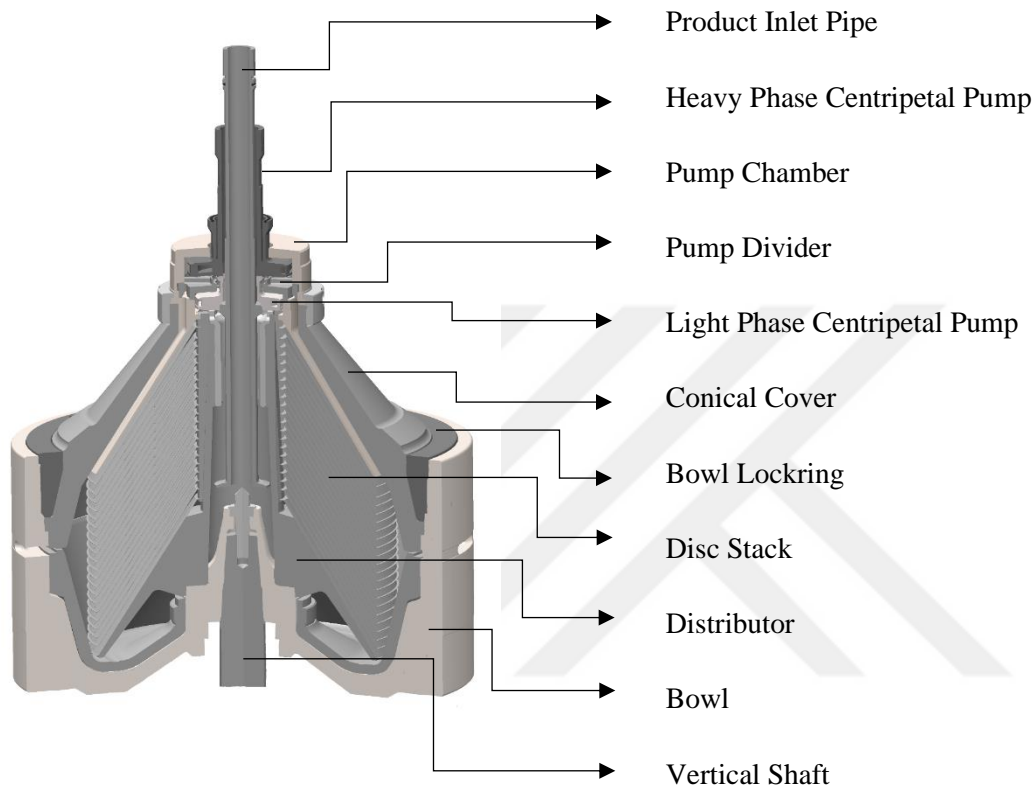


Figure 3.1: Cross section view of the bowl group of a Maxcream 30T centrifugal separator. (Courtesy of HAUS Centrifuge Technologies, 2019).



Figure 3.2: The distributor with a disc stack on it.

Disc stack consists of closely spaced discs (Figure 3.2) and they create a huge surface area for centrifugation. Note that the disc stack also provides a laminar flow region.

3.2 Determination of the Main Factors Influencing the Power Consumption

Centrifugal separators consist of an electric motor, a frame construction, a drive mechanism and a bowl group (rotor). The power generated by motor is transmitted through the belt drive mechanism by motor pulley and vertical shaft. Rotation of the bowl group maintained as a result of the vertical shaft is connected to a bowl group. A control panel (electrical panel-MCC) is a must have equipment to be able to operate a centrifugal separator. The frequency inverter inside the control panel connects to and drives the electric motor of the centrifugal separator. Efforts to reduce the power consumption of centrifugal separators can begin by investigating the reasons of power consumption without forgetting their complex structures.

When we divide the power consumption of the centrifugal separators into sub parts, many factors come to the fore. In order to increase efficiency, the most appropriate of these factors should be determined and necessary changes should be made. Determining the factor that will increase the efficiency of a centrifugal separator can be a difficult task due to the number of factors, but with this approach the most effective factor will become apparent. Theoretically, the following factors may be listed to improve efficiency.

- Windage: Air friction caused by high speed rotation of the bowl group.
- Mechanical Losses: Inefficiencies of the bearings and the belt drive mechanism.
- Flow Losses: Applying rotational force to load kinetic energy on the fluid for separation purpose.
- Electrical Losses: Inefficiency of the electric motor, variable frequency drive (VFD) and other electrical equipment.

Thus, the distribution of power consumption can be expressed as;

$$P_{total} = P_{windage} + P_{mechanical} + P_{flow} + P_{electrical} \quad (3.1)$$

Before getting into the calculation of power losses, knowing the power consumption rate of centrifugal separators would be helpful. Centrifugal separator consumes considerable amount of power, while running it is empty. During separating fluids, centrifugal separator's power consumption rises. The effect of flow rate on power consumption for the testing separator can be seen in the

following graph. The power consumption values have been taken from a product datasheet (HAUS, R&D Team, 2019).

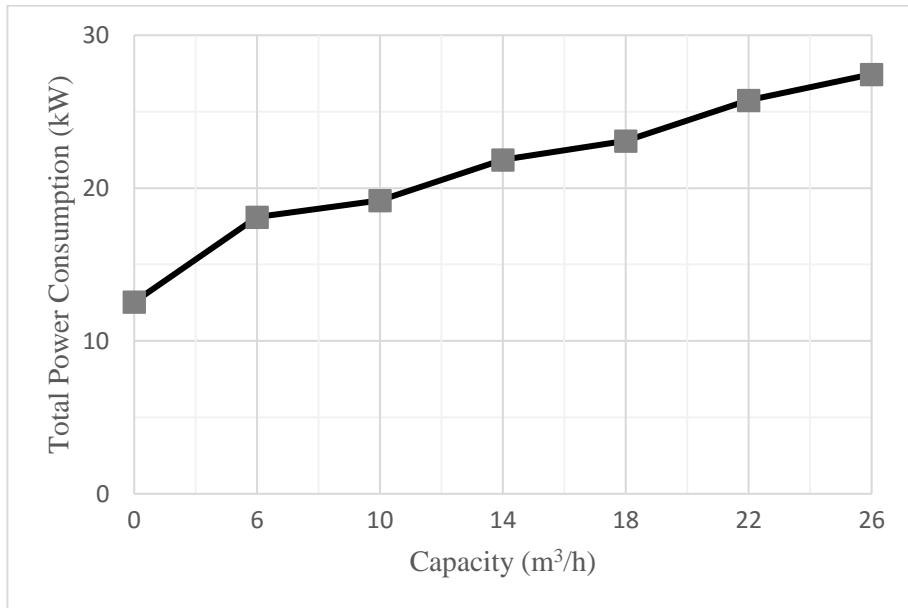


Figure 3.3: Power consumption rate of a standard dairy separator at different flow rates. (Courtesy of HAUS Centrifuge Technologies)

For this study, the total power consumption during separating fluid will be taken as 27.85 kW at a flow rate of 26 m³/h at 2 bar pressure, and it is confirmed on field test as well.

When dividing the power consumption of a separator into smaller parts, the following equation can be found.

$$P_{total\ consumption} = P_{idle} + P_{flow} + P_{electrical} \quad (3.2)$$

3.2.1 Idle Power Consumption

Idle power consumption consists of energy losses due to air friction and mechanical losses such as the use of belt drive mechanism. Flowrate or product type have no effect on it and this consumption is easily readable on the VFD display.

Before getting into determination factors it would be helpful to know idle power consumption of a centrifugal separator.

$$P_{idle} = P_{windage} + P_{mechanical} \quad (3.3)$$

3.2.1.1 Power loss due to air friction (windage)

One of the factors of power losses in separators is the air friction as known as windage effect. High speed rotation of the bowl group is causing a windage effect which can be considered as an element of idle power consumption because the flow does not change the magnitude of the effect. To understand the windage effect a simplified drawing of the testing separator has been shared and the air turbulence has been showed in that Figure 3.4 as red arrows between the bowl and the upper case.

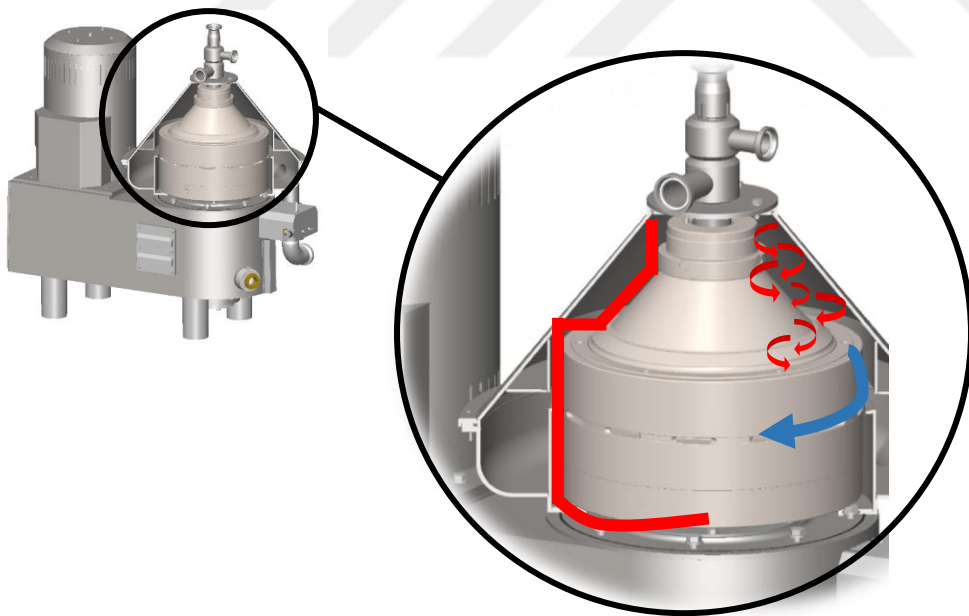


Figure 3.4: Exterior of the bowl group of the testing separator centrifugal separator divided into sub parts.

Aerodynamical drag forces for turbulent flow of rotational bodies can be explained in theory but the bowl group has a complex shape and to make precise estimation, the exterior of the bowl group should be divided into sub parts. The bowl areas to

be subdivided are marked with red lines in the Figure 3.4. After the determination of these sub parts, aerodynamical drag should be calculated for every one of them.

For calculation, the parts would have to be defined as a flat disc or cylindrical models. Then the calculation of each region will yield a total frictional force which would be close estimation on paper. Frictional torque of a rotational body for turbulent flow can be expressed as;

$$dM = c_f * \rho * \omega^2 * \pi * r^3 * \frac{dr}{\cos\theta} \quad (3.4)$$

and,

$$M = c_f * \frac{\rho * \omega^2 * \pi}{5 \cos\theta} * (R_1^5 - R_2^5) \quad (3.5)$$

From this one can derive the power losses of aerodynamical frictions for disc and cylindrical geometries. For flat disc, $\cos\theta$ would be equal to 1 and the formulae can be expressed as;

$$P_{disc} = c_f * \frac{\rho * \omega^3 * \pi}{5} * (R_1^5 - R_2^5) \quad (3.6)$$

From here the equivalent formulae for cylinder can be found as;

($\cos\theta = H/(R_1 - R_2) = 0$, $R_1 - R_2 \rightarrow 0$, l'Hospital rule)

$$P_{cylinder} = c_f * \rho * \omega^3 * \pi * H * (R_1^4 - R_2^4) \quad (3.7)$$

The C_f (coefficient of friction) value for turbulent flow on flat disc surfaces is often quoted in the literature as;

$$C_f = 0.074 * Re_L^{-\frac{1}{5}} \quad (3.8)$$

Because of the complex geometry and to not to go beyond the scope of the study, the windage effect will be gathered by different approach. For the sake of simplicity of calculation, the bowl group can be considered as a rotor consisting of a cylinder and two discs. Then the windage effect would be;

$$P_{rotor} = 2 * P_{disc} + P_{cylinder} \quad (3.9)$$

and the equation for bowl group can be expressed as;

$$P_{rotor} = \frac{2 * \pi * \rho * \omega^3 * R^5 * C_f}{5} \quad (3.10)$$

The coefficient of friction is quoted as $C_f = 0.0075$ in literature (J. M. Owen & R. H. Rogers, 1989).

3.2.1.2 Mechanical losses

Mechanical losses have one of the fair average hits on the power consumption and it has to be calculated. Usage of a flat belt drive mechanism instead of a gear drive mechanism in centrifugal separators provides more efficiency. Although efficiency is increased by using the belt drive mechanism, it still causes power losses. The bearings which has been used in the separator is also another cause of the mechanical losses, but they are mandatory for effective operation. This leaves behind only the belt drive mechanism to inspect for mechanical power losses.

Efficiency of the Tangential Flat Belt

The traditional centrifugal separators were using gear drive mechanisms to speed up the bowl (rotor)group. With advancements in technology, newer and more efficient drive mechanisms are used in centrifugal separators. The centrifugal separators which uses belt drive mechanism has been outnumbered the separators that uses drive gear mechanism. Along with belt drive mechanism, more efficient direct drive mechanisms are developed to reduce energy consumption of separators. Still the belt drive is the most common driving mechanism among the centrifugal separators as of current year because of the high cost of the direct drive motors.

The belt drive power transmission can be seen in the Figure 3.5 as a simplified drawing. The difference in the pulley diameters determines the transmission ratio. The tensions of the belt on each side of the mechanism are T_1 and T_2 respectfully.

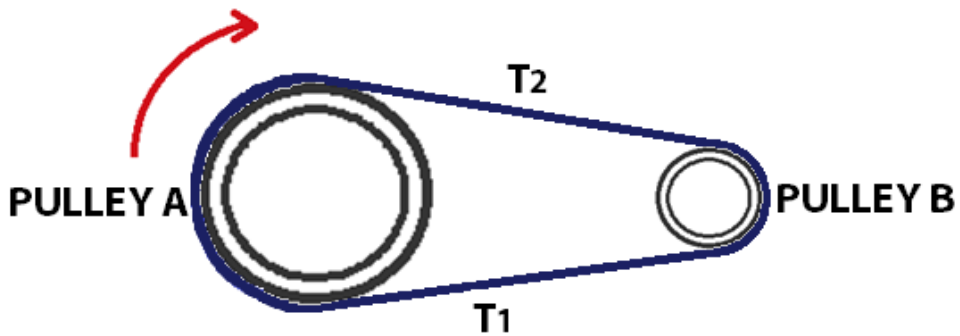


Figure 3.5: Belt drive mechanism

Considering that the pulley rotates clockwise the slack side of the belt expressed as T_1 and the tight side of the belt is expressed as T_2 . The transmitted power on each pulley can be expressed as;

$$\frac{F_1}{F_2} = e^{(\mu_b * \theta_a)} \quad (3.11)$$

and the transmitted torque is;

$$T_a = r_a * (F_1 - F_2) \quad (3.12)$$

A belt drive mechanism consists of two pulleys and a tangential flat belt. It is more efficient than a traditional gear drive mechanism due to low mechanical losses, but the efficiency of the belt drive depends on a few different factors. The main factors affect the efficiency of the belt drive are listed below.

- Friction
- Heating
- Slipping
- Rigidity of the belt (bending)

Every belt has a rigidity and it is depending on the material and the manufacturing method of the belt. One of the operating costs of belt drive is spending energy to bend the belt in spite of its rigidity. It causes a torque loss, so the efficiency will be different among the belt models and brands. During a power transmission a portion of energy will be lost as the belt generates heat. The friction can be seen as a negative factor in belt drive mechanisms because it determines the value of

generated heat, but inadequate friction means no power transmission. Even without the other factors, the tension of the belt itself can affect the power consumption greatly. Inadequate belt tension causes slipping which cause the belt to not transmit power for a short period of time. The slipping effect can be inspected by using a speed sensor. Instant decreases in speed (rpm) during operation means slipping is occurred and the belt tension is not enough.

Because of centrifugal separators high operating speed, another factor becomes important and must be taken into account when designing a system with a belt drive. That factor is the centrifugal force itself, which affects the belt tension on a negative side. The speed of the belt drive can be calculated as follows;

$$v = r * \omega \quad (3.13)$$

and;

$$\omega = \frac{2\pi}{t_{cm}} \quad (3.14)$$

which determines the centrifugal force that acts on the belt;

$$P_c = m_b * v^2 \quad (3.15)$$

Due to the centrifugal force affecting the belt, the belt tensions will be reduced at high speeds. Because of the steadiness of the system, tightness of a newly assembled belt can be misleading. The centrifugal force must be considered and well calculated during the design stage of systems which uses belt drive power transmissions. Therefore, the reduced belt tension due to centrifugal force can be expressed as;

$$\frac{F_1 - P_c}{F_2 - P_c} = e^{(\mu_b * \theta a)} \quad (3.16)$$

The efficiency of the belt drive mechanism can be measure to a degree by inspecting the transmitted torque as follows.

$$\eta = \frac{(T_{out} * n)}{(T_{in} * n)} * 100 \quad (3.17)$$

Small belts cause a high tension, so that the efficiency is reduced by friction. On the other hand, larger belts may appear more efficient in terms of power, but slippage may occur, which may result in unbalanced power transmission. Optimal belt tension for a system should be calculated and well tested for maximum efficiency. Calculating the efficiency of the belt drive system is a very complex process and generally simple assumptions can be made for progress. In this study, literature values were used in order not to go beyond the scope of the study. The efficiency of the flat belt drive was considered 98%. Power consumption will be calculated by using assumptions for mechanical and electrical losses.

3.2.2 Flow Losses

In order to achieve the desired levels of separation, the liquid mixture fed to the bowl without radial speed must reach the bowl speed. According to the separator configuration, the kinetic energy of the kinetic energized liquid is either completely lost after separation or some of it is recovered by centripetal pump. Different configurations are available for centrifugal separators to choose like free inlet/outlet and centripetal pump (paring disc) outlets. In free flow configurations, the kinetic energy imparted to the liquid at the liquid outlets is completely lost. Some centrifugal separators can inherit a centripetal pump which pumps the processed product under pressure, by using the rotating energy of the fluid. The centripetal pumps are designed to convert kinetic energy of the liquid to hydrostatic pressure, in these types, some of the kinetic energy is recovered, but the conversion is not that efficient. The friction between the rotating processed product and the centripetal pump is so high that the conversion efficiency is very low. Most of the rotating energy is lost to friction.

This section will be discussed under the title of power recovery. Friction losses in the distance traveled by the liquid in the bowl are omitted. With this assumption, we can accept flow losses as angular momentum losses.

Energy consumption due to angular momentum

Theoretically the angular momentum can be expressed by following equations;

$$\dot{L} = r * \dot{p} \quad (3.18)$$

\dot{p} : linear momentum [$kg * m * s^{-2}$]

$$\dot{p} = \dot{m} * v \quad (3.19)$$

Thus;

$$\dot{L} = \dot{m} * v * r \quad (3.20)$$

and

$$v = \omega * r \quad (3.21)$$

v : speed [$m * s^{-1}$]

angular momentum becomes this;

$$\dot{L} = \dot{m} * \omega * r^2 \quad (3.22)$$

mass per unit can be expressed as;

$$\dot{m} = \rho * v * A \quad (3.23)$$

and the flowrate,

$$Q_v = v * A \quad (3.24)$$

Q_v : volumetric flowrate [$m^3 * s^{-1}$]

$$\dot{m} = \rho * Q_v \quad (3.25)$$

$\dot{m} = [kg * s^{-1}]$

$$\dot{L} = \rho * Q * \omega * r^2 \quad (3.26)$$

\dot{L} : angular momentum $kg * m^2 * s^{-2}$

Then the power loss of a rotating liquid becomes;

$$\dot{L}\omega = \rho * Q * \omega^2 * r^2 \quad (3.27)$$

3.2.3 Electrical Losses

Even though the centrifugal separator is a mechanical machine, the motor and the sensors on it needs electricity to work. A control panel (electric panel/motion control center-MCC) (Figure 3.6) is shipped together with a centrifugal separator to be able to operate it. The control panel has a PLC (programmable logic controller) and HMI to control the separator easily. Sensors on the separator transmits data through cables to PLC and the data values can be read at HMI. Speed sensor and a vibration sensor is placed on the separator to measure such values for safety reasons. While operating; control panel's components heats up by time as electrical power is lost by conversion to heat. This power consumption will also be counted as electric losses but Control panel itself is another reason of power consumption of a separator, but it is out of this studies scope.



Figure 3.6: The components of electrical panel

A Frequency inverter allows to increase motor speed gradually and the speed of the inverter can be changed through the control panel. A speed-time chart can be prepared to understand the frequency inverter.

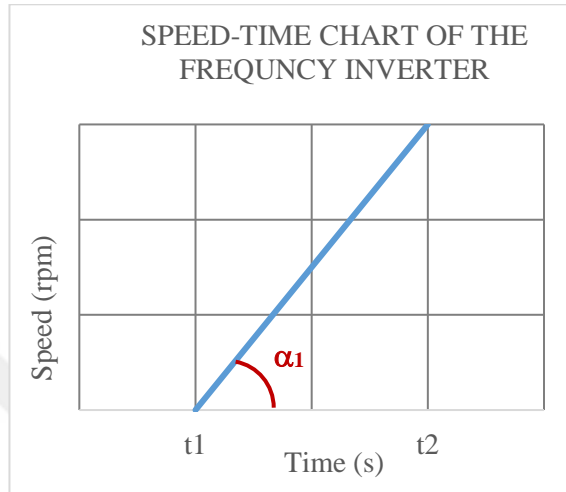


Figure 3.7: Speed-time chart of a VFD (high)

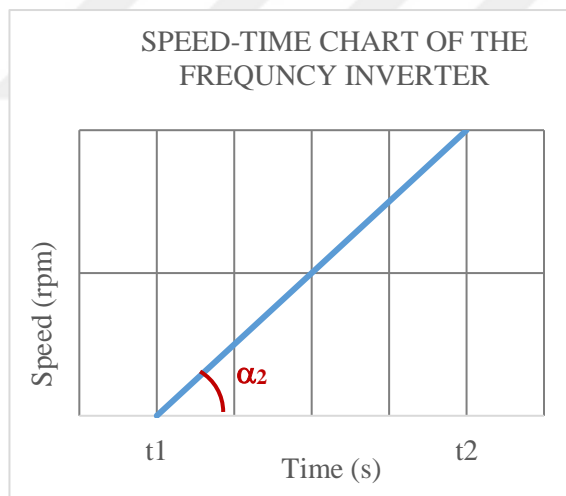


Figure 3.8: Speed-time chart of a VFD (low)

The α shows the inclination of the line (Figure 3.7, Figure 3.8). The frequency inverter allows to set how long the motor will reach to the operating speed, so that the value α will be greater if the frequency inverter is set to reach operating speed in less time. The moment of inertia of the bowl cause a high draw of electrical current. Change of a setting of the frequency inverter can be effective in power consumption but most of the separators can manage to reach operating speed in 15 minutes. Because of that, not much reduction can be achieved by changing VFD parameters.

Electrical motor of the testing separator is driven by a Danfoss FC301 P45K VFD which is placed on middle of the electrical panel. The VFD's efficiency is 98% (Danfoss, last accessed December, 2019) and it will be helpful to calculate power loss. The main power source of the separator is a WAT brand 45 kW electrical motor. The electrical motor was working on 48.4% Hz at operating speed. The efficiency can be taken as 93% during operating with fluid and 91.9% during idle operation (Figure 3.9).

V	Hz	min ⁻¹	kW	Cosφ	A	η	S.F.:1.15 Load Efficiency
380	50	1470	45	0.85	86.9	IE2-93.1%	%50 91.9%
440	60	1765	51.8	0.85	84.6		%75 93.0%

Figure 3.9: Label of the electrical motor

3.3 Theory of Centripetal Pump

One of the main parts of a centrifugal separator is a centripetal pump. The centripetal pump is a requirement for many centrifugal separators operating in industrial applications because of the ability to pressurize phases and use a cleaning in place (CIP) system to clean the internal volume of the machine. The centripetal pump can be described as a centrifugal pump impeller which standstill during the operation. In various centrifugal separator models, centripetal pumps (also known as paring discs) are used for pressurizing the phase prior to taking it out. Centripetal pumps are also a necessity to use modern cleaning techniques such as Cleaning in Place (CIP). The bowl and the continuous medium inside it rotate at high speed and the generated kinetic energy is converted to pressure by centripetal pumps. An energy loss occurs during this conversion because of the friction between the continuous medium and centripetal pump.

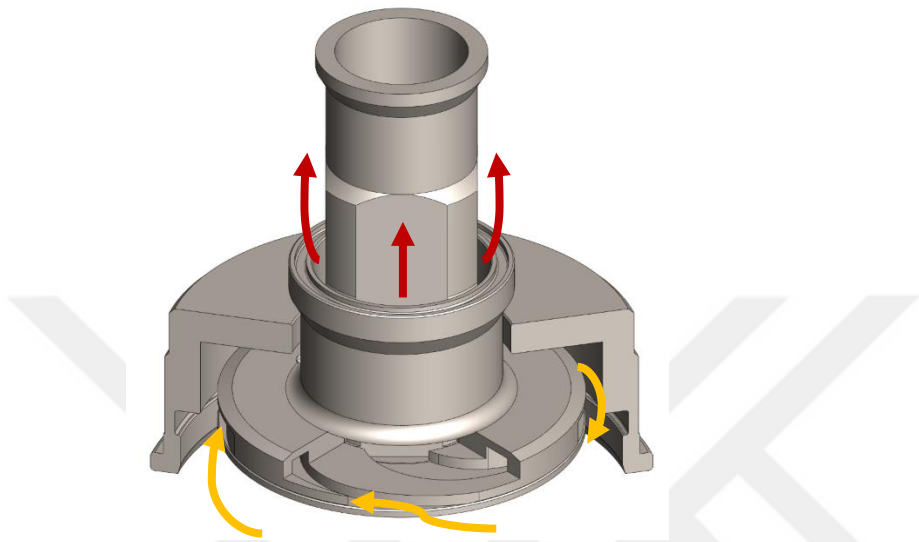


Figure 3.10: A centripetal pump and the flow. (HAUS Centrifuge Technologies, 2019)

The Bernoulli equation utilized in this study to calculate the approximate amount of power generated/regained by stationary centripetal pump accessory is essentially a relation between pressure, velocity, and elevation, and is valid in regions of steady, incompressible flow where net frictional forces are negligible. In our case, since the distance between the inlet and outlet of this stationary pump (Figure 3.10, Figure 3.11) is relatively close (max. 200mm), power loss due to elevation is neglected.

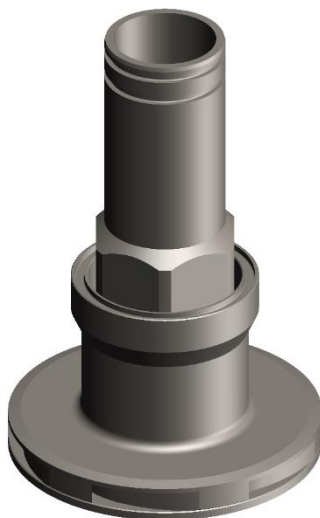


Figure 3.11: The stationary centripetal pump

Despite the fact that it is more frequently utilized in pressure drop calculations through conventional tubing-piping installations, heat exchangers, pump and turbines etc., the approach and mindset in this thesis study show an analogous nature. Therefore, it became a proper tool in calculating stationary pump potential. The Bernoulli equation is derived through the conservation of linear momentum principle, with its usefulness and limitations.

The key to successfully deriving the Bernoulli equation is through assuming the viscous effects are relatively small compared to inertial, gravitational and pressure effects. Although all fluids have viscosity at a certain degree, the viscosity assumption cannot be valid for every point of any flow domain. This draws a limit to the validity of the Bernoulli equation, no matter how ineffective the real viscosity of that certain fluid is. However, it is also a fact that, at some specific ‘regions’ of flow domain, where this approximation on the viscosity become reasonable. However, it is important to underline that these ‘regions’ are by no means cancel out the effects of the viscosity, but on the contrary, they are domains where the viscous forces are ‘negligible’ in comparison to other forces acting on the fluid.

Frictional and viscous forces are always very important near the wall regions of flow domain, especially there is some kind of movement, therefore interaction between a fluid and a solid is involved in the engineering problem. In this study, this problem is avoided by defining ‘no-slip’ boundary conditions on each of the walls and assigning a very good defined mesh near the boundaries. This approach allowed the Bernoulli equation to provide reliable results in terms of power regeneration through employing a specific accessory, the stationary centripetal pump.

When the motion of a fluid particle through a flow field in steady flow is considered and Newton’s second law (which is referred to as the linear momentum equation in fluid mechanics) is applied in the arbitrary s -direction on a particle moving along a streamline gives;

$$\sum F_s = ma_s \quad (3.28)$$

In flow region inside of a centrifuge separator and in the vicinity of centripetal pump device, the frictional forces relatively low and therefore negligible and there

is no heat transfer between the medium and the peripherals. However, there is vigorous movement of the fluid around the centripetal pump. Under these circumstances, the significant factors acting in the s -direction on the pump inlet are the flow energy due to pressure difference and kinetic energy due to circular movement of the fluid. Therefore, following equation can be formed:

$$P dA - (P + dP)dA - W \sin \theta = mV \frac{dV}{ds} \quad (3.29)$$

where θ is the angle between the normal of the streamline and the vertical z -axis at that point, $m = \rho V = \rho dA ds$ is the mass, $W = mg = \rho g dA ds$ is the weight of the fluid particle, and $\sin \theta = dz/ds$. Substituting,

$$-dP dA - (\rho g dA ds) \frac{dz}{ds} = \rho dA ds V \frac{dV}{ds} \quad (3.30)$$

Canceling dA from each term and simplifying,

$$-dP - \rho g dz = \rho V dV \quad (3.31)$$

Noting that $V dV = \frac{1}{2} d(V^2)$ and dividing each term by ρ gives,

$$\frac{dP}{\rho} + \frac{1}{2} d(V^2) + g dz = 0 \quad (3.32)$$

Integrating,

$$\int \frac{dP}{\rho} + \frac{V^2}{2} + gz = \text{constant} \quad (3.33)$$

In the case of incompressible flow, the first term also becomes an exact differential, and integration gives

$$\frac{P}{\rho} + \frac{V^2}{2} + gz = \text{constant} \quad (3.34)$$

As the final form of the Bernoulli equation under the assumptions previously stated. It is commonly used in fluid mechanics to define and assess steady, incompressible flow along a streamline for inviscid regions of flow. The value of the constant in Equation. 3.34 can be evaluated at any point on the streamline where the pressure, density, velocity, and elevation are known. The Bernoulli equation in this case can also be written between the inlet (Equation 3.34₁ and Equation 3.34₂) for same streamline as (steady-incompressible flow):

$$\frac{P_1}{\rho} + \frac{V_1^2}{2} + gz_1 = \frac{P_2}{\rho} + \frac{V_2^2}{2} + gz_2 \quad (3.35)$$

We recognize $V^2/2$ as kinetic energy, gz as potential energy, and P/ρ as flow energy, all per unit mass.

3.4 Field Test Unit

The testing separator is settled in HAUS Centrifuge Technologies R&D testing field. Test setup equipment can be seen at Figure 3.12.



Figure 3.12: The testing setup in R&D Testing Field

The product inlet line has been connected to the feed pump. Product inlet and heavy phase outlet has manometers. Heavy phase line is also connected to a diaphragm valve to apply counter pressure. Light phase line is open to an atmosphere and not a manometer or a diaphragm valve connected. Because of separators structure the light phase line and the light phase centripetal pump have not been used. The heavy phase centripetal pump is capable of 26 m³/h at 4 bar pressure flow before the light phase centripetal pump touch the product. Water will be pumped from a tank into the separator by a pump.

The pump speed is adjustable via VFD (Figure 3.13). Maximum frequency is 50 Hz and at maximum frequency the pump is capable of feeding about 35 m³/h. The frequency of the feed pump can be read from the VFD screen.



Figure 3.13: The VFD of the feed pump.

A flowmeter (Figure 3.14) is attached to the feed line. The power consumption data has been collected at different flowrates. The flowrate has been watched for about a minute to make sure the flow is stable. Values are collected after the flow was continuously stable.



Figure 3.14: A photograph of the flowmeter.

A manometer with a gauge from -1 bar to 5 bar has been selected for product inlet line to measure the pressure in case of a vacuum happens. The manometer on the heavy phase has been selected with a gauge from 0 bar to 10 bar to be able to read high pressures when increase the pressure by using the counter pressure valve.

The test has been conducted with three centripetal pump designs at 6 m³/h, 10 m³/h, 14 m³/h, 18 m³/h, 22 m³/h and 26 m³/h flowrates. At each flowrate the outlet pressure has been adjusted to 2 bars. In maximum flowrate, the values have been collected at 1.5 bar, 2 bar, 2.5 bar, 3 bar, 3.5 bar and 4 bar outlet pressures.

The centripetal pumps designed in three size that is 150 mm, 160 mm and 170 mm diameter (Figure 3.15). Smallest and the biggest centripetal pumps has 6 channels and the middle one has 3 channels for the fluid to get into it.



Figure 3.15: Centripetal pumps before assembling the separator.

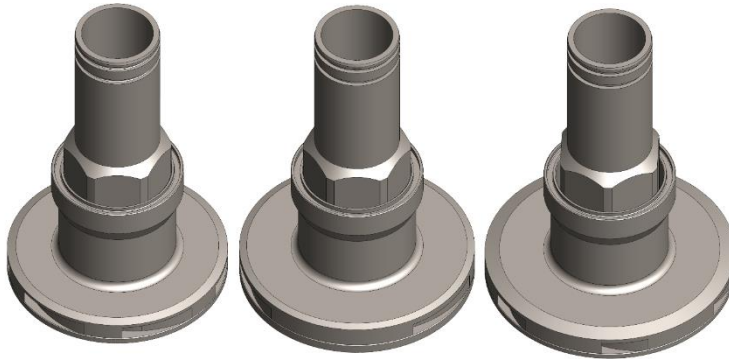


Figure 3.16: 3D Models of the centripetal pumps

This configuration is specifically chosen to inspect the effects of different centripetal pump designs (Figure 3.16). The Ø150 mm and the Ø170 mm centripetal pump will be compared to inspect the effects of the diameter. However, the Ø160 mm centripetal pump will be compared to other centripetal pumps for inspection of the effects of channel quantity.

3.5 Centripetal Pump Simulations in CFD

3.5.1 Problem Definition

In this study, a comprehensive CFD approach is developed to carry out pressure loss and power retrieval through alternative centripetal pump designs located at the outlet of an industrial disk-stack separator. A single-phase, uniform medium (water), the density, temperature and viscosity of which is assumed to be constant through the flow region. This fundamental approach made the application of Bernoulli equation possible towards calculating the actual power retrieval from the data that CFD solver generates under defined boundary conditions (BC).

The differences between the three alternatives of centripetal pump designs are observed in their outer diameters (150, 160 and 170 mm), number of channels (6, 3 and 6, respectively) and the channel curvatures (Figure 3.17).

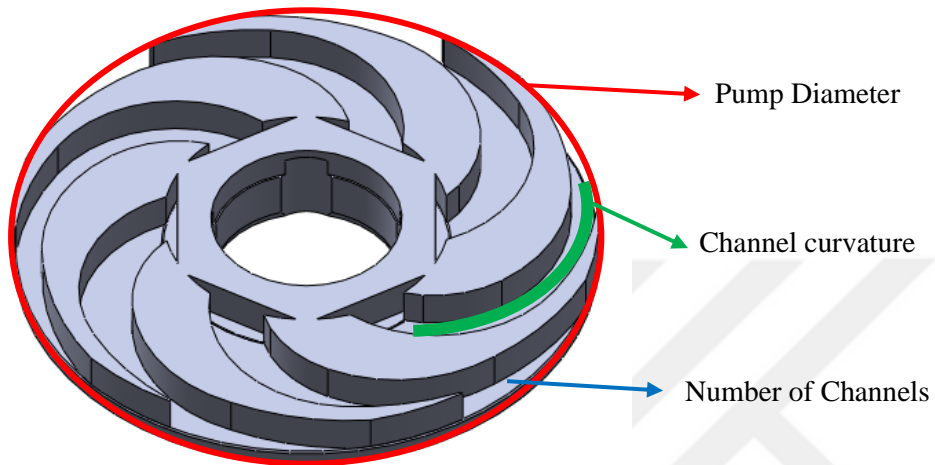


Figure 3.17: Cross section of a centripetal pump.

Throughput rates varying between $6 \text{ m}^3/\text{h}$ and $26 \text{ m}^3/\text{h}$ are applied in the form of normal velocities (given that the density is constant) on the inlet boundaries to every 3D model, the secondary and tertiary operations of which are implemented in SolidWorks CAD environment and ANSYS Design Modeler. Results from surface average monitoring for normal velocity and gage pressure on the outlet surface of models are harvested from the CFD solver. These data later become pressure loss result and power retrieval calculation through Bernoulli equation.

The 3D models of centripetal pumps and the channels can have been shared in order to understand the difference (Figure 3.18).

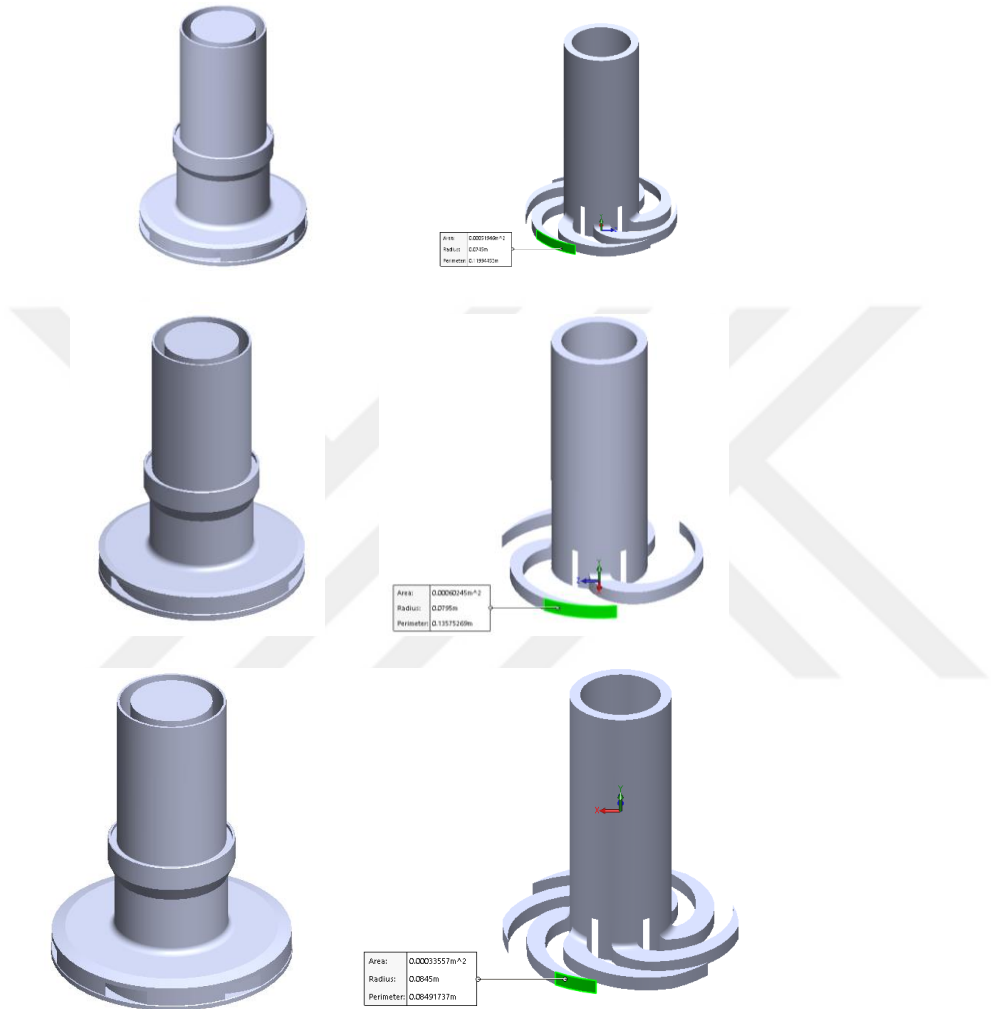


Figure 3.18: The 3D models of centripetal pumps and the difference in channel designs.

Product inlet areas for each of the centripetal pumps has been shared in the Table 3.1.

Table 3.1: The areas are collected from the measure feature of the Solidworks CAD software.

Centripetal Pump Model	Inlet Flow Area of the Centripetal Pump
Ø150 mm centripetal pump	0.00051946 m ²
Ø160 mm centripetal pump	0.00060245 m ²
Ø170 mm centripetal pump	0.00033557 m ²

3.5.2 Model Properties

As stated previously, 3D model preparation is conducted in a CAD-CAE (Computer Associated Design-Computer Associated Engineering) correspondence. A Boolean operation called ‘fill’ to prepare flow region through centripetal pump assembly is employed, avoiding a possible Fluid-Solid Interface (FSI) between the medium and the original accessory. This measure is taken as the FSI investigation is not significant and assuming an FSI will contradict the assumption that the flow is Bernoulli-applicable. Total volume preparation involves four steps, and the steps are as follows;

- CAD data is translated into the ANSYS Design Modeler,
- Boolean ‘Fill’ feature is run, and all peripheral features of the solid model is omitted,
- Remaining partitions from the Boolean operation is trimmed in CAD environment,
- Final 3D model is imported back in the Design Modeler, after which the meshing and solver setup is commenced.

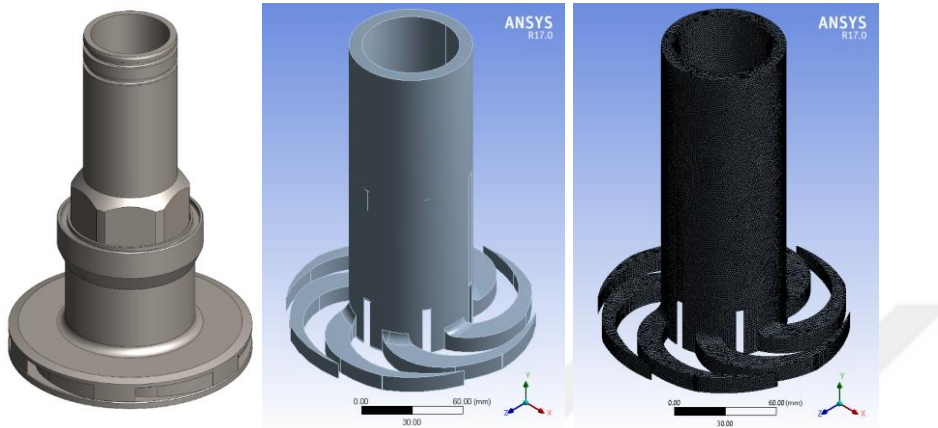


Figure 3.19: CFD model evolution from SolidWorks CAD to meshing.

As seen on Figure 3.19, the entire region of centripetal pump filled-up by the medium is considered. That is, the wet volume, involving the surfaces represented by the solid construction through the centripetal pump is adopted directly from the model. Dimensional properties and the intricate internal structure are therefore loyal to the commercial product. An alternative of this application would be sectioning the whole geometry as studied elsewhere (Ekin, 2019), leaning on the fact that the pump blades and volute is symmetrical around the axis.

3.5.3 Mesh Structure

Due to the intricate nature of the volute and the blade geometries, in constructing the finite element group, tetragonal elements are preferred over a mixed/custom selection of elements and especially hexa-dominant elements. Utilizing hexa-dominant or multizone meshing algorithm may result in poor aspect ratio and orthogonal quality, two essential parameters to a successful mesh.

Second concern of implementing the ‘correct’ mesh structure, is that the trade-off between the conversion character and time consumption of a typical steady-state simulation. There, meshing time (from mere minutes to weeks, in some applications) should be considered as a part of solver time itself. To satisfy a time-efficient analysis along with the converging ability of simulations, a size range between 0.01 mm and 3 mm is adopted with 1.5 mm max. face size. The resulting mesh for 150 mm model, along with orthogonal quality and skewness of elements are summarized are seen on Figure 3.20. Also, high smoothing with fast transition,

hence fast adaptation of mesher to rapidly changing curved geometry of the models. A detailed table of mesh characteristics can be seen on Table 3.2.

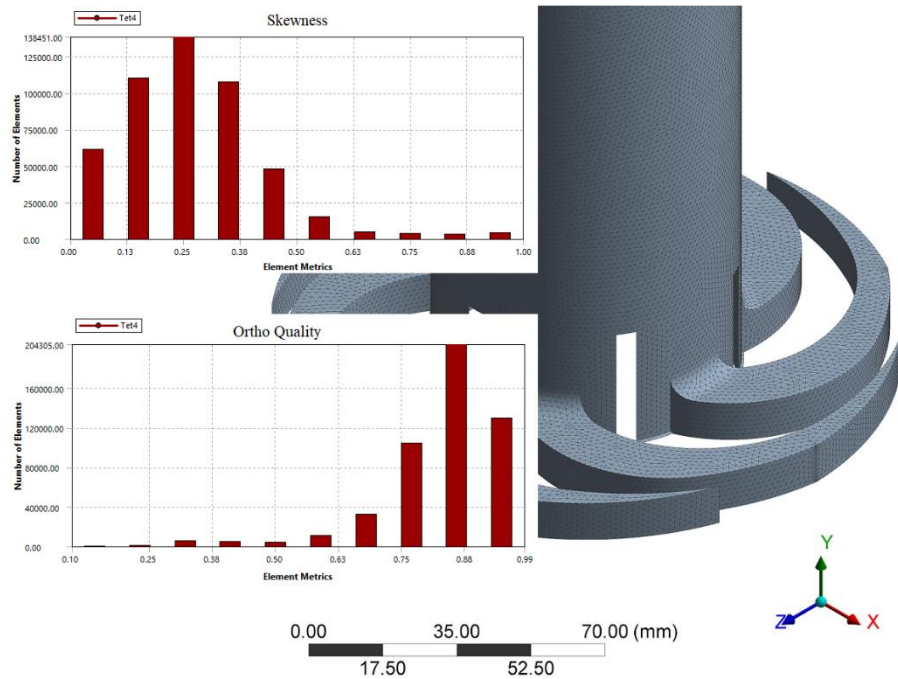


Figure 3.20: Mesh characteristics of 150 mm diameter, six channel centripetal pump with tetra mesher.

Table 3.2: Mesh properties applied to each model.

<i>Property</i>	<i>Value</i>
Nodes	112769
Elements	495105
Element Mid-side Nodes	Dropped
Sizing Properties	
*Sizing Function	Curvature only
*Relevance Center	Fine
*Smoothing	High
*Transition	Fast (Growth Rate: 1.850)
*Span Angle Center	Fine
Curvature Normal Angle	18° (as Default)
Element Size Range	
*Min Size	0.01mm
*Max Face Size	1.50mm
*Max Tet Size	3mm
Defeaturing	Yes
*Tolerance	0.005mm

3.5.4 CFD Setup on Fluent Solver

In the course of this study, both experiments and the simulation use water as process medium, as there is no limiting factor of amount, season or content in operating on water for a centrifuge machinery. Its viscosity and density, along with cost efficiency can replace and represent, for testing purposes, any medium (milk, olive oil, mineral oil etc.) that is actually processed through the machine. As per standard material library of ANSYS Fluent, its density is 998.2 kg/m^3 and viscosity 0.001003 Pas .

A Moving Reference Model (MRF) is adopted to represent rotational movement of a typical centripetal pump. Since the relative movement of fluid and pump impeller resemble a reasonable analogy, the impeller reference frame is rotated at a rate of 5800 rpm, that is the nominal rotational speed of the machine. BC's defined as 'wall' are also registered as rotational due to MRF modeling requirements, but their rotational speed is set to 'Relative to Adjacent Cell Zone' to prevent a non-zero relative speed between the model geometry and the actual model boundaries.

'Operating Conditions' are defined as 1 atm operating pressure, and -although insignificant compared to relative centrifugal force, -9.81m/s^2 . Specified operating density is defined to be equal to that of water, as there are no secondary and tertiary phases involved. Solution methods selected are summarized on Table 3.3.

Table 3.3: Solution methods group utilized through the simulations.

Solver Parameter	Value
Pressure Velocity Coupling	SIMPLE
Spatial Discretization	
Gradient	Least Squares Cell Based
Pressure	Second Order
Momentum	Second Order Upwind
Turbulent Kinetic Energy	First Order Upwind
Specific Dissipation Rate	First Order Upwind

MRF model tends to diverge at high angular rates, especially when the overall and local mesh quality fails to satisfy convergence demands of the model. Although at lower rates applied (at 100 rpm-500 rpm range) solver behavior was convergent, getting results from nominal speed of 5800 rpm could not be achieved. As increasing the mesh quality, refining or adding local applications will increase computational force required and not generally practical, the solution to divergence problem is searched for elsewhere. As a result, the Momentum default (= 0.7) in Under-relaxation Factors (URF), was reduced gradually and at 0.1, convergence was achieved through the mesh structure previously described at 10^{-3} absolute criteria. Remaining factors are left as default in URF panel under Solution Controls tab.

Solver is initialized with Standard Initialization every time. Since the main BCs are inlet velocity (hence the throughput rate) and counter pressure at the outlet and these values vary at different simulation sets, the computation is started from either inlet or outlet boundaries. Through this approach, the number of input parameters per simulation are kept at '1'. As a standard route, ANSYS Fluent calculates initialization values of the domain automatically. It is important to emphasize that every parameter left at its 'default' value in the CFD interface is calculated and not fixed to an exact point. Knowing this, the Turbulent Kinetic Energy [m^2/s^2] and Specific Dissipation Rate [1/s], specific to $k - \Omega$ turbulence model, are left as default, to be calculated and reassigned in the very second iteration. A typical initialization scheme for 2.3219 m/s inlet velocity BC and 4 Bar outlet pressure BC is given in Table 3.4.

Table 3.4: Standard initialization values for nominal speed and pointwise simulation parameters

Initialization Parameter	Value
Gauge Pressure (Bar)	0
x- Velocity (m/s)	-1.198238×10^{-6}
y- Velocity (m/s)	9.739602×10^{-7}
z- Velocity (m/s)	3.461268×10^{-6}
Turbulent Kinetic Energy [m^2/s^2]	7.697858
Specific Dissipation Rate [1/s]	766101.9

Number of limitations during steady-state simulations are limited to 250. Transient scheme is avoided since there is no particulate phase therefore no time-dependency. That the machine is operated at a constant rate of feed and constant rate of rotation. Majority of analyses are converged at around 175 iterations, as seen on Figure 3.21. Although 10^{-3} overall convergence tolerance is debatable, the comparison of simulation results to field tests prove that the simulation settings are sufficient.

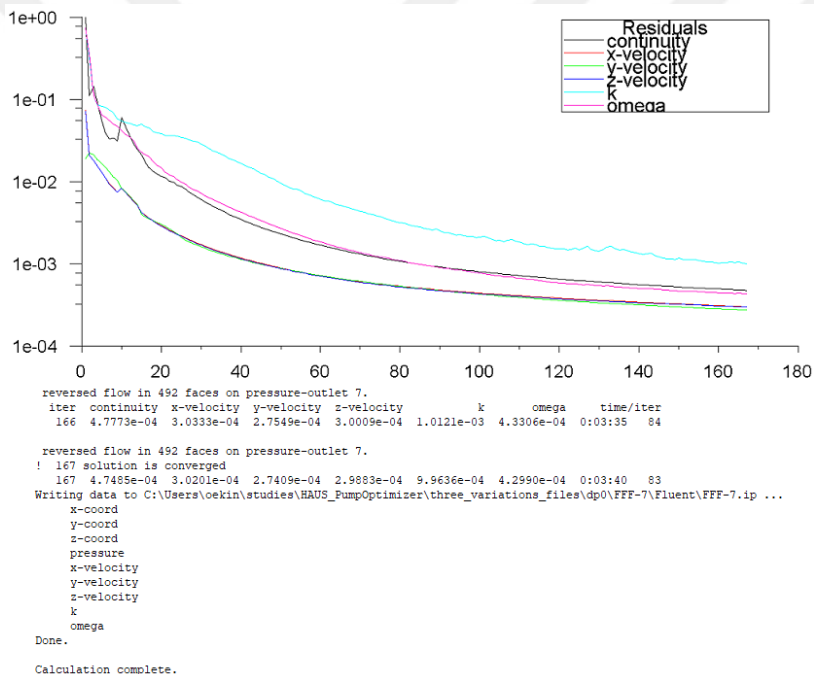


Figure 3.21: CFD Solver residual monitor at the step of convergence

The computational aspect of this study is to reveal the amount of power recycled through a stationary centripetal pump installation located on the axis of revolution of centrifugal separator. This, being an internal element of the procedure, is a fail-safe operation to eject clarified medium from inside the separation volume. However, similar to that of particle separation characteristics, how effective this accessory works is obscure for an observer due to implicit nature of operation. CFD fills this exact gap by calculating (approximately) how much of the power spent in the entire process is recovered by using this apparatus. Data from simulations integrated with the additional figures on power consumption analysis is provided in the results section.

4 RESULTS AND DISCUSSIONS

4.1 Main Factors of Power Consumption

Field test has been done at HAUS R&D Department Test Center in three steps. The centrifetal pumps with a diameter of 150 mm, 160 mm and 170 mm tested respectively. Only one step of test has been done in one day to make sure environment temperature or other factors does not interfere with the results. Changing of an environmental condition have not been observed. Before every test, the equipment of the testing field such as flowmeter and feed pump had been checked. Also, idle power consumption value has been checked before every configuration to make sure centrifetal pump diameter has no effect on idle power consumption. As mentioned earlier graph the separator consumes 12.55 kW during operating without product. During testing the power consumption value has been collected from VFD interface. For every configuration, same testing procedure has been applied.

During field test, power consumption values has been collected carefully. The flowrate and the outlet pressure have been checked for 30 seconds to 1 minute before taking the value. This action has been taken to gather more accurate power consumption values. After the test results has been taken for each configuration, the following graphs are generated with the collected values.

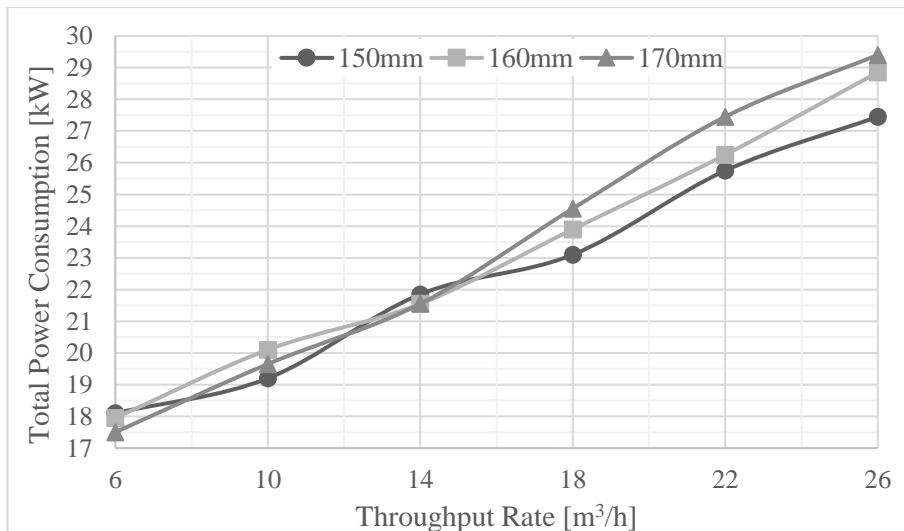


Figure 4.1: Power consumption of centrifetal pump variations at 2 bar counter pressure

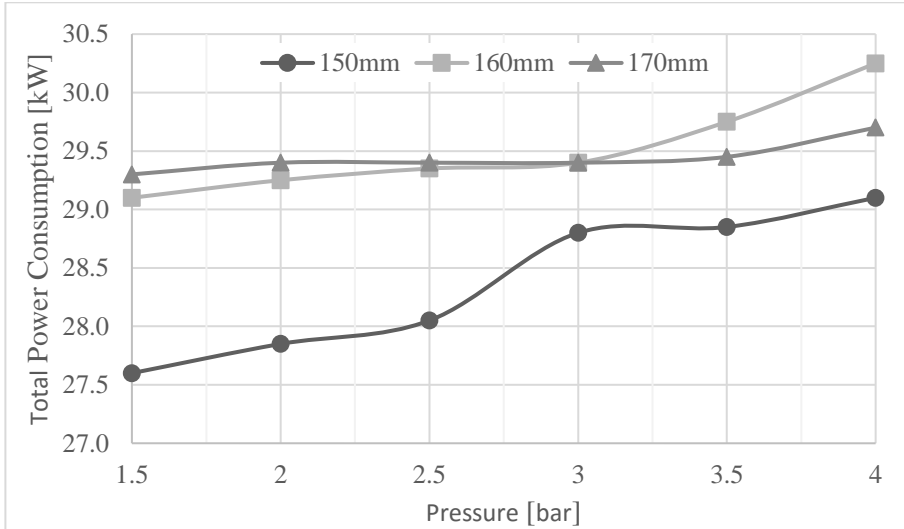


Figure 4.2: Power consumption of centripetal pumps at 26 m³/h throughput rate

Power loss due to air friction (windage)

In view of the optimized shape of the bowl group, the coefficient of friction was calculated as 0.006. The aerodynamical drag for the testing separator can be calculated by using the P_{rotor} formula (equation 3.10).

Windage effect on the testing separator can be calculated by using below values;

$$\omega = 5800 \text{ rpm (operating speed)} = 607.06 \text{ rad/s}$$

$$r_b = 0.34 \text{ m (outer radius of the bowl)}$$

$$\rho = 1.127 \text{ kg/m}^3 \text{ (density of air at } 40^\circ\text{C (Cengel, Y. \& Cimbala, J., 2018))}.$$

$$P_{windage} = 8.64 \text{ kW}$$

Mechanical losses

For mechanical losses $P_{mechanical}$ formula can be generated from Equation 3.3 as shown below;

$$P_{mechanical} = (P_{idle} - P_{windage} - P_{electrical, idle}) \quad (3.36)$$

$$P_{mechanical} = 2.53 \text{ kW}$$

Flow is ineffective of the magnitude of the air friction(windage) so the power consumption when the separator is operating but not processing fluid (P_{idle}) would include the air friction losses. Because of the VFD's and other component specifications are known, the power consumption due to air friction can be excluded from the idle power consumption can express the mechanical power loss.

Mechanical losses seem to be small compared to other major losses such as windage and flow.

Flow loss due to angular momentum

To calculate the angular momentum losses of the testing separator's centripetal pump ($\varnothing 150$ mm), following data has been used.

r_c : 71.4 mm = 0.0714 m (minimum radius of the water layer on the centripetal pump chamber)

ρ : 992.1 kg/m³ (density of water at 40°C (Cengel, Y. & Cimbala, J., 2018))

ω : 607.06 rad/s

Q: 26 m³/h

Q₂: 26/3600 = 0.00722

Thus, flow losses can be calculated from Equation 3.27,

$$P_{flow} = 13.46 \text{ kW}$$

When the results of field tests conducted with three centripetal pump designs were examined according to both capacity and pressure changes, it was found that both the centripetal pump outer diameter and the number of channels affected the flow-induced energy consumption in parallel with the results of CFD analysis. Separator energy consumption; The $\varnothing 170$ mm centripetal pump seems to cause 5.9% more power consumption than the $\varnothing 150$ mm centripetal pump. It was observed that the number of centripetal pump channels should be determined according to the capacity and pressure value of the liquid to be pumped. Figure 4.2 shows that energy consumption increases dramatically, especially at high counter pressures.

Electrical losses

$$\eta_{electrical} = \eta_{VFD} * \eta_{motor} \quad (3.37)$$

$$\eta_{electrical,total} = 0.91 \text{ (motor efficiency is chosen for 75\% load)}$$

$$\eta_{electrical,idle} = 0.90 \text{ (motor efficiency is chosen for 50\% load)}$$

$$P_{electrical} = P_{total} * \frac{1 - \eta_{electrical}}{\eta_{electrical}} \quad (3.38)$$

$$P_{electrical,total} = 2.71 \text{ kW}$$

$$P_{electrical,idle} = 1.38 \text{ kW}$$

The power consumption distribution on determined capacity and pressure rate for every factor listed in the table below. The Table 4.1 will be used for determination of the main factor.

Table 4.1: Distribution of power consumption factors

Factor	Value
P _{flow}	13.46 kW
P _{windage}	8.64 kW
P _{mechanical}	2.53 kW
P _{electrical}	2.71 kW
P _{total}	27.34 kW

The testing separator's total power consumption was 27.85 kW on determined capacity that is 26 m³/h and pressure rate is 2 bar on field test. The calculation gives 27.34 kW. This deviation is 1.8% and is disregarded. After the inspection of factors has been done, the following distribution graph was obtained.

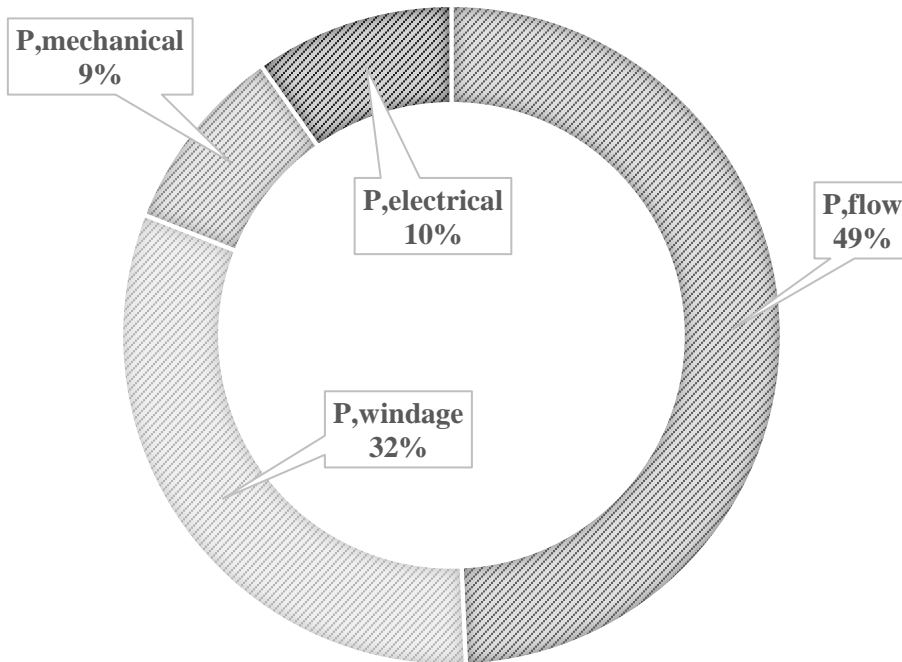


Figure 4.3: Distribution of Power Consumption of the Testing Separator

The most contributing factor to power consumption was found to be the flow losses. Since the flow losses depends on the angular momentum, centripetal pump design has been found to be the most important factor to be changed in terms of reducing power consumption. For understanding the effects of centripetal pump on power consumption a testing system for different centripetal pumps has been structured and tested.

4.2 Validation of Power Recovery Through the Centripetal Pump

Due to the availability of validation procedure specific to centripetal pump through the study, a CFD model developed targeting the upwind calculation through this accessory. Two aspects were investigated in the course of this study. Firstly, and since there is no specific data for the inlet of the centripetal pump, a set of

simulation runs were conducted to discover the inlet pressure values once the inlet velocities calculated through the equation of continuity. Once these data are determined, CFD software can handle the inlet properties of a homogenous fluid.

Secondly, and as stated previously in the method section, possible power recovery through centripetal pump, for three different variations of centripetal pumps actively manufactured and installed in the centrifugal separators were investigated by numerical analysis.

Centripetal pump is recovering some of the flow power by pressurizing the fluid. Therefore, the power recovery of designed 3 centripetal pumps will be compared after calculating the recovery rate by help of CFD.

As stated previously, CFD results may asserted as remarkable, only when a proper validation can be delivered. In this instance and the context of this study, this verification comes off the stability and repeatability of simulations at an acceptable convergence tolerance.

When the continuity convergence criteria are assumed to be 10^{-3} as common practice, the simulation for each centripetal pump design converges at around two hundred iterations. As a supporting aspect, the pressure and velocity distributions along the three models are given in Figures 4.4 and 4.5. General stability of results also the convenience between field data stream and outlet surface averages on pressure and velocity indirectly satisfy the simulation validity. The velocity graph is naturally calculated, given the original inlet velocity values as “Boundary Conditions”. In pressure distribution graphics however, default values of pressure values in the inlet region are directly assumed. This approach enables the user to determine the unknown value by the set of iterations allowed.

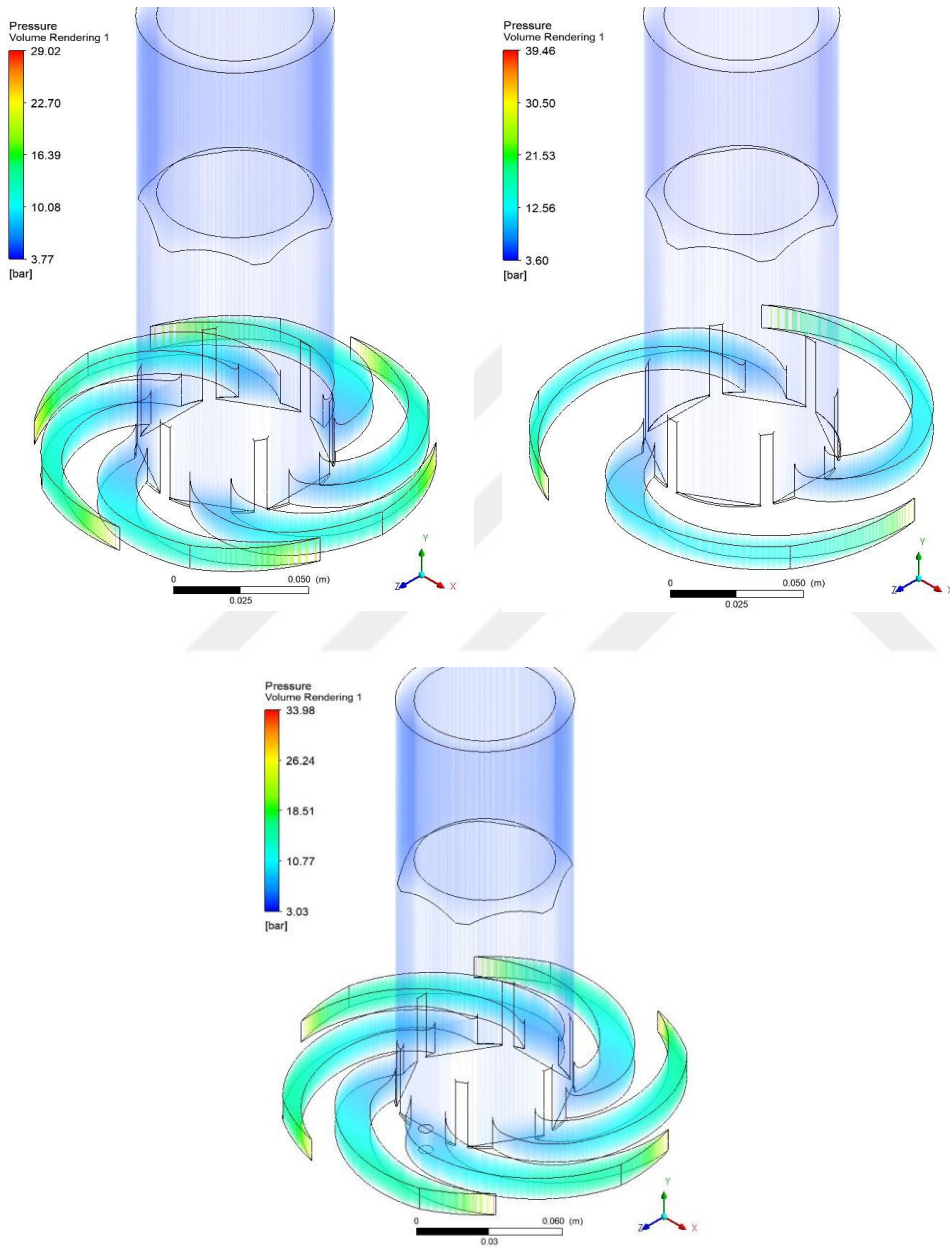


Figure 4.4: Pressure distribution through 150 mm (top, left), 160 mm (top, right) and 170 mm centripetal pump designs in $k-\Omega$ RANS model.

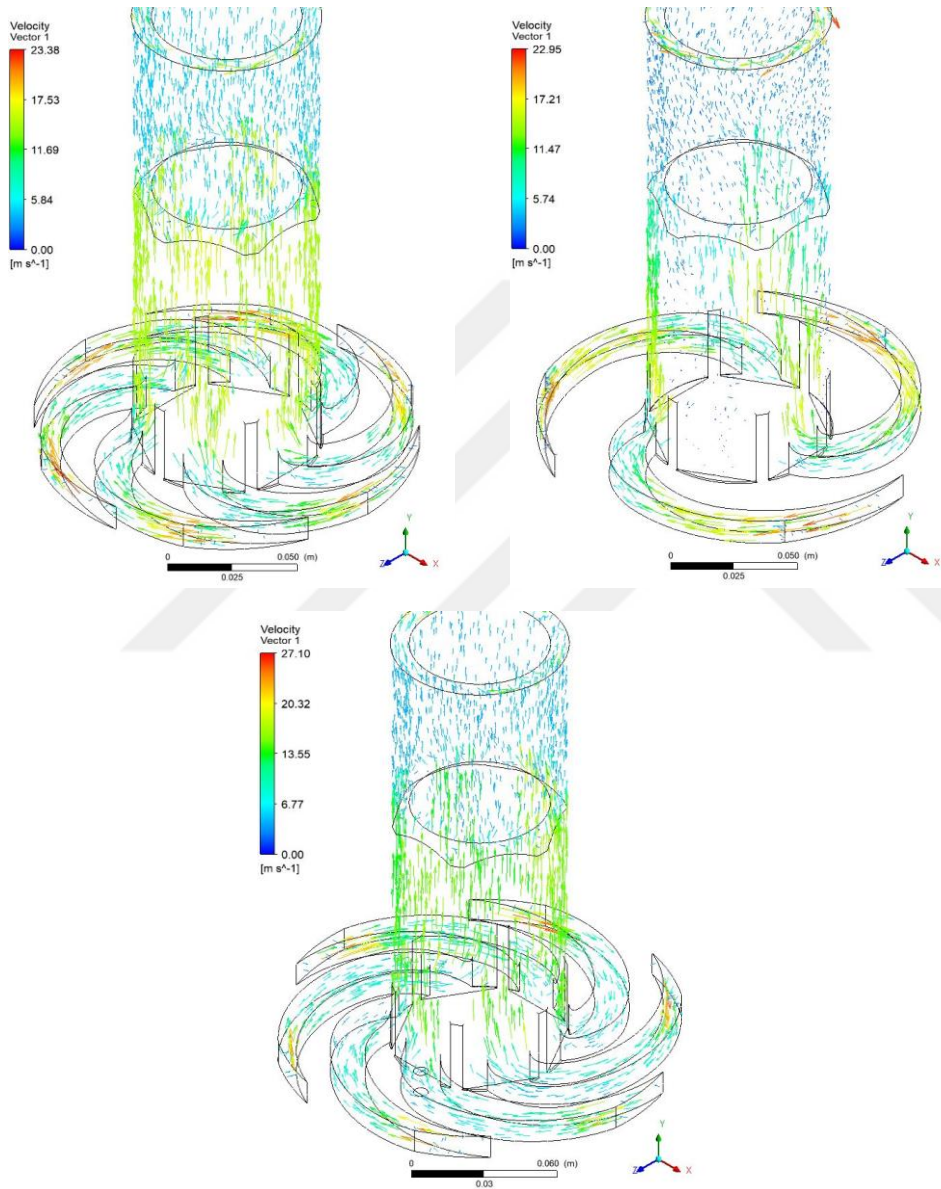


Figure 4.5: Vector graph for velocity distribution along 150 mm (top,left), 160 mm (top,right) and 170 mm centripetal pump designs in $k-\Omega$ RANS model

Through calculating the inlet pressure values by the help of CFD solver (defining inlet velocity B. C's and leaving pressure on surfaces as default values) the inlet pressures are calculated. This way, theoretical results for pressure loss can now be calculated and suggested as seen in Figure 4.6. Pressure loss, or rather pressure transformation tends to increase as throughput rate is increased towards $26 \text{ m}^3/\text{h}$.

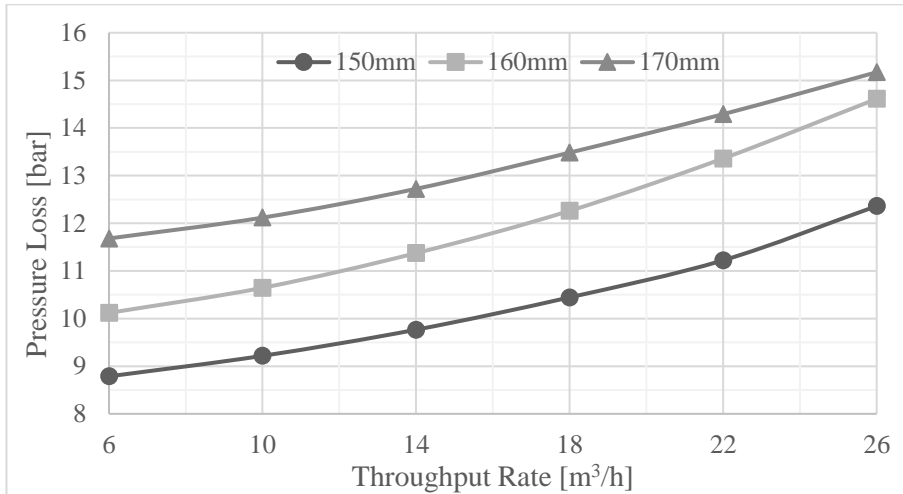


Figure 4.6: Pump pressure losses at 2 bar counter pressure

On the contrary, pressure loss is only mildly affected by the increase in the counter pressure applied. This is expected as the main factor determining the pressure loss, thus the inlet pressure is the volumetric flow through the pump, which in the Figure 4.7, fixed at 26 m³/h.

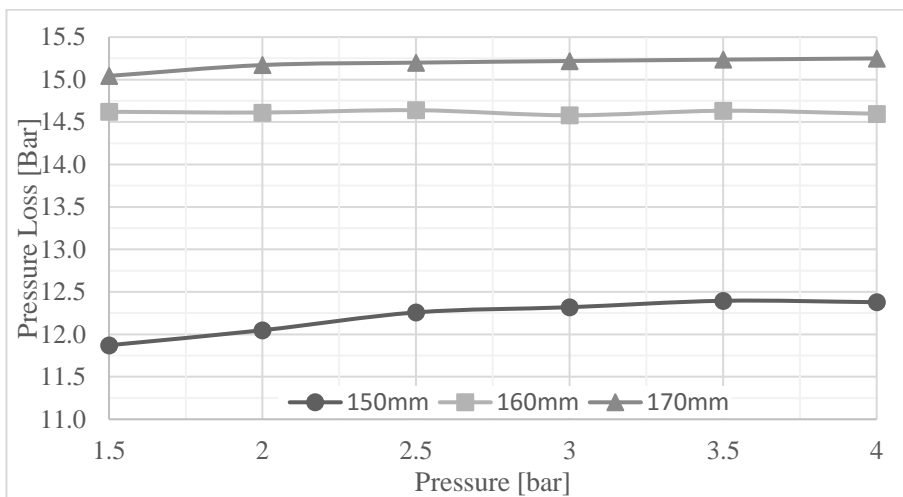


Figure 4.7: Pump pressure losses at 26 m³/h throughput rate

The main feature of the CFD analysis implemented in this study is to offer a convenient basis for the power recovery from the centripetal pump, an important asset in centrifuge design and benchmarking. From this point of view, power recycled from different types of pumps utilized tend to improve when a 6-channel

model is preferred over a 3-channel model, as seen with 150mm and 170mm models in both Figure 4.8 and 4.9. Regardless of the volumetric flow rate (Figure 4.8) or counter pressure applied (Figure 4.9) number of channels utilized in the model outweighs the pump outer diameter. Again, from this perspective, the advantages attributed to the centripetal pump employment in centrifugal separators is better earned when models with correct flow division are utilized.

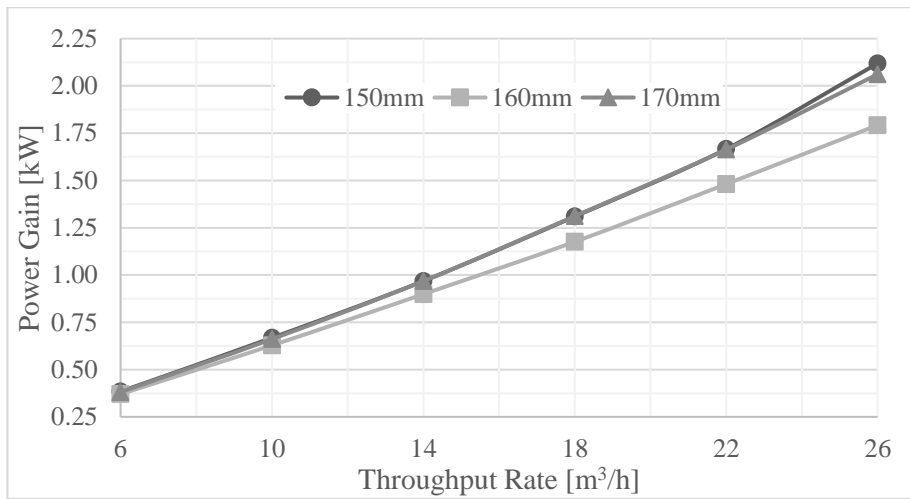


Figure 4.8: Power recycled from centripetal pumps at 2 bar counter pressure

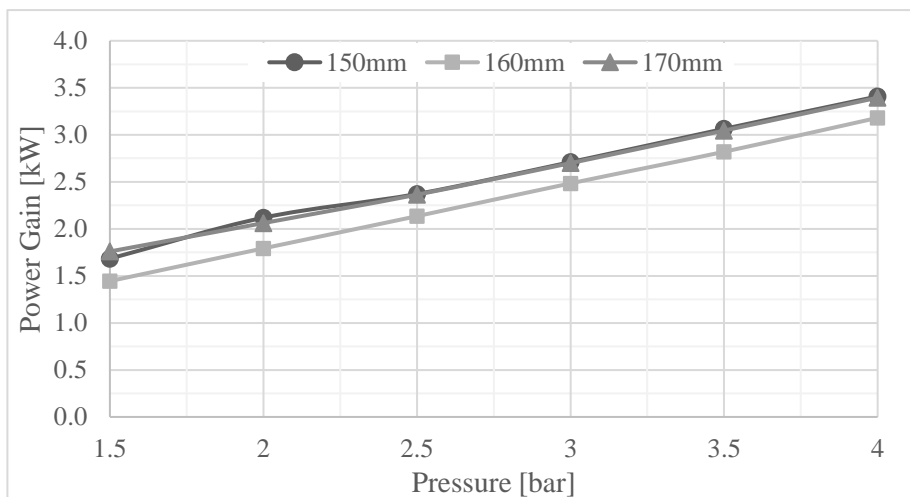


Figure 4.9: Power recycled from centripetal pumps at 26 m³/h throughput rate

The testing results has shown a relation between power consumption and the centripetal pump design.

It can be observed by inspection of the calculation that the centripetal pump diameter is directly affects the power loss due to angular momentum. Also, Practical and theoretical results have shown that the power consumption of a centrifugal separator may vary depending on the design of the centripetal pump. With the increase of centripetal pump diameter an increase in the ability to pressurize more fluid by centripetal pump has been observed. It is also observed that using a centripetal pump at its capacity limit reduced the power consumption compared to bigger diameters.

Therefore, the recycled power can be calculated for centripetal pumps that recovery rates are founded by help of CFD and field test results. It has shown that selection of the correct centripetal pump diameter is crucial for power recovery. In determined capacity and pressure rate; Ø150 mm centripetal pump is the most suitable design for all respect. Its power recovery rate is between 11.5% to 21.2% as seen in the Figure 4.10.

With this approach, it has been determined that the selection of the minimum number of channels and the minimum diameter of the pump to provide the required hydrostatic pressure to transport the liquid to the next station minimizes the flow-induced energy consumption.

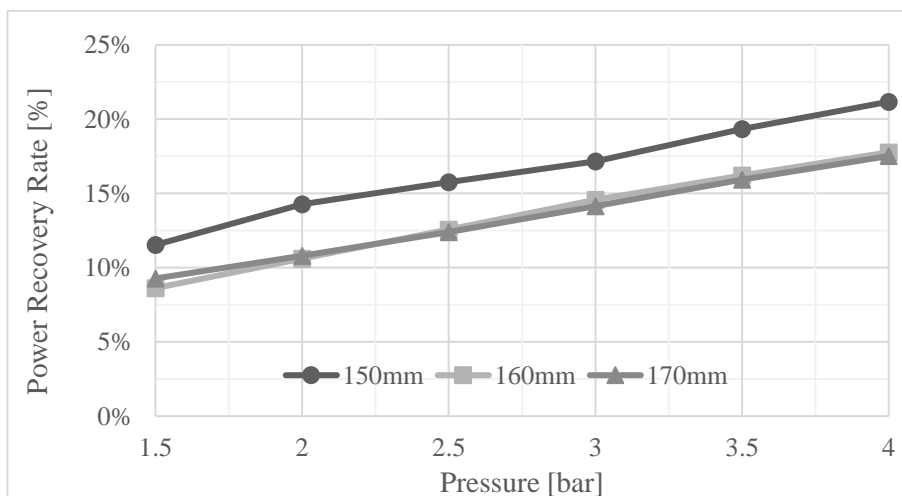


Figure 4.10: Recovered power by centripetal pumps at 26 m³/h throughput rate

5 CONCLUSION

Centrifugal separators are one of the most useful but power-hungry devices of the industry. Their high-tech safety equipment and high operating speed can make processes easier, but they come with a price, huge energy bill. Because of its supreme power consumption, many applications are not suitable to work with a separator. Very few studies have been developed to make centrifugal separators more efficient in a way that make them popular in newer industrial fields. Field experiences shows that the power consumptions change between 1.2 kWh m^{-3} and 1.5 kWh m^{-3} .

In this study, centrifugal separator power consumption is analyzed under four main categories and parameters under each category are studied in detail. It has been found that 32% of the total power consumption is spent to overcome the air friction on the outer surface of bowl group, 9% to mechanical losses and 10% to electrical losses. It was found that the power consumption to accelerate the flow was the largest, accounting for 49% of the total consumption. The main factor to be used in the study of reducing power consumption due to angular momentum without reducing the separation efficiency is the liquid discharge diameter, that is, the outer diameter of the centripetal pump. The results of the test confirmed that the effect of the outer diameter was consistent with the theoretical calculation. If a free outlet centrifugal separator was used, the average power consumption would be 1.12 kWh m^{-3} . It has been reduced to 0.99 kWh m^{-3} with the $\text{Ø}150 \text{ mm}$ centripetal pump. In other words, 12% reduction in power consumption has been achieved.

In addition, the determination of the main factors of power consumption will shed light on which parameters will be focused in the subsequent power consumption reduction studies. It is theoretically possible to reduce the total power consumption to below 0.5 kWh m^{-3} by focusing on the following issues in future studies.

- Energy losses due to air friction correspond to 32% of the total consumption. Considering that the bowl diameter and radial velocity cannot be changed, which is one of the most important design criteria for the separation process, studies on reducing friction coefficient and air density can be done in order to reduce air friction in future studies.

- Another approach to reduce the power consumption of a centrifugal separator might be changing the electrical motor. In this study a 45kW IE2 class electrical motor was used and the efficiency of it is 91% with using a belt drive mechanism. Instead of the IE2 class electrical motor, more efficient IE4 class electrical motor could be used and this would increase the efficiency of the drive system to at least 93% ('The Association of Electrical Mechanical Trades', last accessed December, 2019). The efficiency can be increased even further by using a direct drive motor. This design change would increase the efficiency to 95%. That increase in efficiency would reduce the electrical consumption drastically in the long run.

REFERENCES

- Bell, G. R. 2013. Analysis and Development of a Decanter Centrifuge. PhD Thesis, University of Canterbury.
- Cengel, Y. & Cimbala, J. 2018. Fluid Mechanics, Fundamentals and Applications 4th ed. New York: McGraw-Hill Education, pp 950-956, ISBN 978-1-259-69653-4.
- Danfoss. 2019. Design Guide VLT® Automation Drive FC301/302. Retrieved from Danfoss: <https://www.danfoss.com/> Last Accessed 10/12/2019
- Ekin, O. 2019. A Thermal-Fluid Investigation of Centrifugal Separation Processes of Multiphase Fluids. PhD Thesis, Adnan Menderes University.
- Friso, D. 2017. Dynamic analysis of centrifugal separator in unsteady-state condition with and without variable-frequency drive. **Contemporary Engineering Sciences**, DOI: 10.12988/ces.2017.611173.
- HAUS, R&D Team. 2019. Internal HAUS Product Data.
- J. M. Owen & R. H. Rogers. 1989. Flow and Heat Transfer in Rotating Disc Systems: Large Clearance, Turbulent Flow Ch. 6.4. New York: John Wiley & Sons.
- Kefalas, P., Margaritis, D. P., 2009. CFD Simulation and Experimental Verification of the Flow Field in a Centrifugal Separator. **International Review on Modelling and Simulation**, 40 pages.
- Khalid, N. 2014. Efficient energy management: Is variable frequency drives the solution. **Procedia - Social and Behavioral Sciences**, 145, 371-376.
- Milledge, J. & Heaven, S. 2011. Disc Stack Centrifugation Separation and Cell Disruption of Microalgae: A Technical Note. **Environment and Natural Resources Research**, 1. 17-24. DOI: 10.5539/enrr.v1n1p17.
- Sutherland, K. 2009. Filtration and separation technology: What's new with centrifuges? **Filtration and Separation**, 46 (3), 30-32.
- Tarleton, E.S. & Wakeman, R.J. 2007. Solid/Liquid Separation: Equipment Selection and Process Design. Oxford: Butterworth-Heinemann.
- 'The Association of Electrical Mechanical Trades'. 2019. IE Motor Efficiency Level Tolerances,. Retrieved from <https://www.theaemt.com/> Last Accessed 10/12/2019.

- Verma, N. M., Mehrotra, S., Shukla, A. & Mishra, B. N. 2010. Prospective of biodiesel production utilizing microalgae as the cell factories: a comprehensive discussion. **African Journal of Biotechnology**, 9(10), 1402-1411, DOI: 10.5897/AJBx09.071.
- Wild, P. M., Djilali, N., . 1996. Experimental and Computational Assessment of Windage Losses in Rotating Machinery. **Journal of Fluids Engineering**, DOI: 10.1115/1.2817488.



RESUME

Personal Information

Name and Surname : Erdem SAĞLAM

Place and Date of Birth : Isparta, 01/04/1988

Education

Undergraduate:

Bursa Uludağ University (2007-2013)

Faculty of Engineering and Architecture

Mechanical Engineering Department

Postgraduate (MSc):

Aydın Adnan Menderes University (2015-2020)

Graduate School of Natural and Applied Sciences

Mechanical Engineering Program

Foreign Languages: English, Spanish

Work Experience

2018 - Present	Separator R&D Manager	Haus Makina Sanayi Tic. AŞ.
2013 - 2018	R&D Engineer	Haus Makina Sanayi Tic. AŞ.

Contact

e-mail:

erdem.saglam@haus.com.tr

Adress:

HAUS Makina Sanayi Tic. AŖ.

ASTİM Organize Sanayi Bölgesi 1. Cadde

No: 110 / Aydın – TÜRKİYE

Phone:

+90 505 666 96 36

14/01/2020

AYDIN